Electronic Supplementary Information (ESI)

An unsual $Ni_2Si_2P_8$ cluster formed by complexation and thermolysis

Christoph G. P. Ziegler,[a] Clemens Taube,[b] John A. Kelly,[a] Gabriele Hierlmeier,[a] Maria Uttendorfer,[a] Jan J. Weigand*[b] and Robert Wolf*[a]

Table of Contents

1. General Information

All manipulations were performed under an atmosphere of dry argon using standard Schlenk techniques or an MBraun UniLab glovebox. Solvents were dried and degassed with an MBraun SPS800 solvent-purification system. THF, diethyl ether, and toluene were stored over molecular sieves (3 Å). *n*-hexane was stored over a potassium mirror. Deuterated solvents (C_6D_6, tol-d_8, THF-d_8) were stirred over potassium, distilled, degassed and stored over molecular sieves (3 Å). The starting materials [(IDipp)Ni(η^2-H_2C=$CHSiMe_3$)$_2$] (IDipp = 1,3-bis(2,6-diisopropylphenyl)imidazolin-2-ylidene), [(IMes)Ni(η^2-H_2C=$CHSiMe_3$)$_2$] (IMes = 1,3-bis(2,4,6-trimethylphenyl)imidazolin-2-ylidene), LSi and [LSi(η^2-P_4)] were prepared according to previously reported procedures.[1–4] The synthesis of [LSi(η^2-P_4)] (L = CH[C(Me)N(Dipp)][C(CH_2)N(Dipp), Dipp = 2,6-*i*$Pr_2C_6H_3$) published by Driess and co-workers was slightly modified as described below.

NMR Spectroscopy:
NMR spectra were measured on a Bruker AVANCE III HD Nanobay (^{1}H (400.13 MHz), ^{13}C (100.61 MHz), ^{19}F (376.50 MHz), ^{29}Si (79.50 MHz), ^{31}P (161.98 MHz)) 400 MHz UltraSield or on a Bruker AVANCE III HDX, 500 MHz Ascend (^{1}H (500.13 MHz), ^{13}C (125.75 MHz), ^{19}F (470.59 MHz), ^{29}Si (99.36 MHz), ^{31}P (202.45 MHz)). All ^{13}C NMR spectra were exclusively recorded with composite pulse decoupling. Reported numbers assigning atoms in the ^{13}C spectra were indirectly deduced from the cross-peaks in 2D correlation experiments (HMBC, HSQC). Chemical shifts were referenced to δ_{TMS} = 0.00 ppm (^{1}H, ^{13}C), δ_{CFCl3} = 0.00 ppm (^{19}F), δ_{TMS} = 0.00 ppm (^{29}Si) and $\delta_{H3PO4(85\%)}$ = 0.00 ppm (^{31}P). Chemical shifts (δ) are reported in ppm. Coupling constants (J) are reported in Hz.
For compounds, which give rise to a higher order spin system in the ^{31}P{^{1}H} NMR spectrum, the resolution enhanced ^{31}P{^{1}H} NMR spectrum was transferred to the software gNMR, version 5.0, by Cherwell Scientific.[5] The full line shape iteration procedure of gNMR was applied to obtain the best match of the fitted to the experimental spectrum. ^1J(^{31}P^{31}P) coupling constants were set to negative values and all other signs of the coupling constants were obtained accordingly.
In a glovebox, 20 mg of the respective compound were dissolved in 0.4 mL of deuterated solvent (tol-d_8 or THF-d_8). The solution was transferred into a *J. Young* valve NMR tube. ^{1}H and ^{31}P NMR measurements were performed in a temperature range from 240 K to 360 K. Throughout the measurement the NMR tube was kept spinning with 20 Hz to obtain a homogeneous solution.

Elemental analysis: Elemental analyses were determined by the analytical department of the University of Regensburg with a Micro Vario Cube (Elementar).

2. Synthetic Procedures

2.1 Modified Procedure for the Synthesis of [LSi(η^2-P_4)]

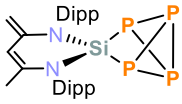

The synthesis of LSi and [LSi(η^2-P_4)] was performed according to a published procedure of Driess and co-workers.[3] However, the synthesis of [LSi(η^2-P_4)] was modified in order to prevent the formation of significant amounts of [{LSi}$_2$(μ-$\eta^{2:2}$-P_4)].
Silylene LSi (6.29 g, 14.1 mmol, 1.0 equiv.) was dissolved in toluene (75 mL). This solution was added dropwise via a dropping funnel to a clear solution of white phosphorus (1.75 g, 14.1 mmol, 1.0 equiv.) dissolved in toluene (30 mL) at 60 °C. The reaction mixture was additionally stirred for 18 h at 60 °C. $^{31}P\{^1H\}$ NMR monitoring subsequently showed the selective formation of [LSi(η^2-P_4)]. Next, the solution was concentrated in *vacuo* to 25 mL. Crystals of [LSi(η^2-P_4)] were obtained after storage at −30 °C over a period of 2 days.

Yield: 6.1 g (76%).

NMR spectroscopic data agree with those reported by Driess and co-workers.[3]

^{1}H NMR (400.13 MHz, 300 K, C_6D_6): δ / ppm = 1.21 (d, $^3J_{HH}$ = 6.7 Hz, 6 H, Dipp: CH*Me*$_2$), 1.37 (d, $^3J_{HH}$ = 6.7 Hz, 6 H, Dipp: CH*Me*$_2$), 1.46 (s, 3 H, L: NC*Me*), 1.51 (d, $^3J_{HH}$ = 6.8 Hz, 6 H, Dipp: CH*Me*$_2$), 1.54 (d, $^3J_{HH}$ = 6.8 Hz, 6 H, Dipp: CH*Me*$_2$), 3.32 (s, 1 H, L: NCC*H*$_2$), 3.61 (sept, $^3J_{HH}$ = 6.8 Hz, 2 H, Dipp-IDipp: C*H*Me$_2$), 3.70 (sept, $^3J_{HH}$ = 6.7 Hz, 2 H, Dipp-IDipp: C*H*Me$_2$), 3.91 (s, 1 H, L: NCC*H*$_2$), 5.21 (s, 1 H, L: γ-C*H*), 6.98-7.36 (m, 6 H, Dipp: 2,6-*i*Pr$_2$C$_6$*H*$_3$).

$^{31}P\{^1H\}$ NMR (161.98 MHz, 300 K, C_6D_6): δ / ppm = ABX$_2$ $\delta(P_A)$ = −348.0 (dt, $^1J(P_A,P_X)$ = −146.8 Hz, $^1J(P_B,P_X)$ = −188.0 Hz, 1P), $\delta(P_B)$ = −342.4(dt, $^1J(P_B,P_X)$ = −144.7 Hz, $^1J(P_A,P_B)$ = −188.0 Hz 1P), $\delta(P_X)$ = 131.9 (dd, $^1J(P_X,P_A)$ = 146.8 Hz, $^1J(P_X,P_B)$ = −144.7Hz, 2P) ^{29}Si satellites: ^1J(Px,Si) =31.5 Hz.

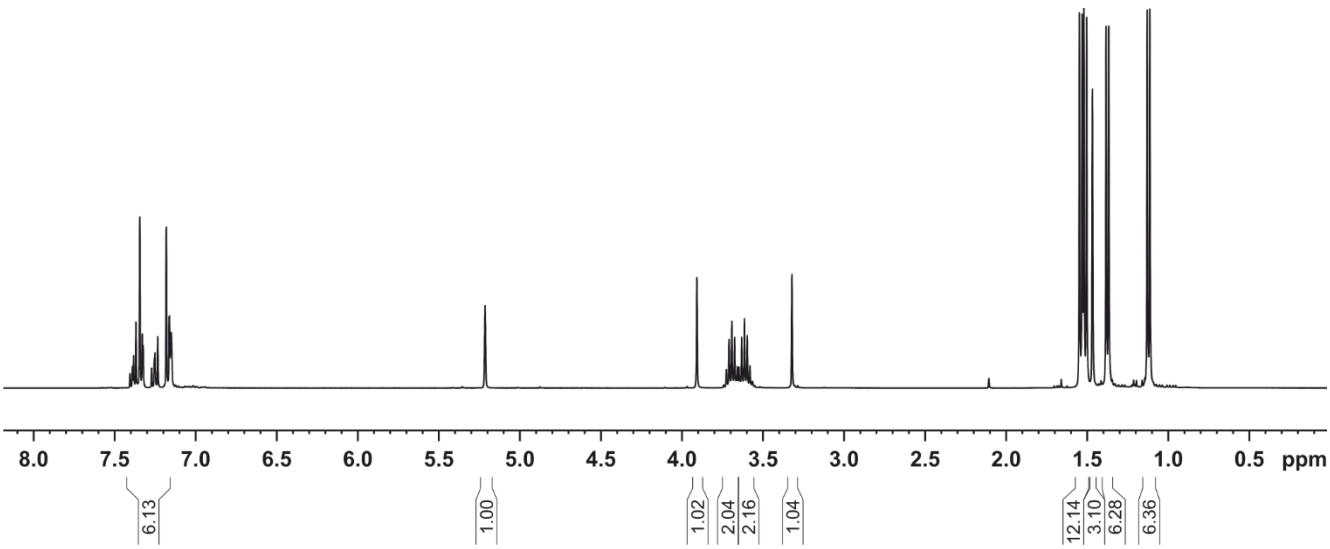

Figure S1. ^{1}H NMR spectrum (400 MHz, 300 K, C_6D_6) of [LSi(η^2-P_4)].

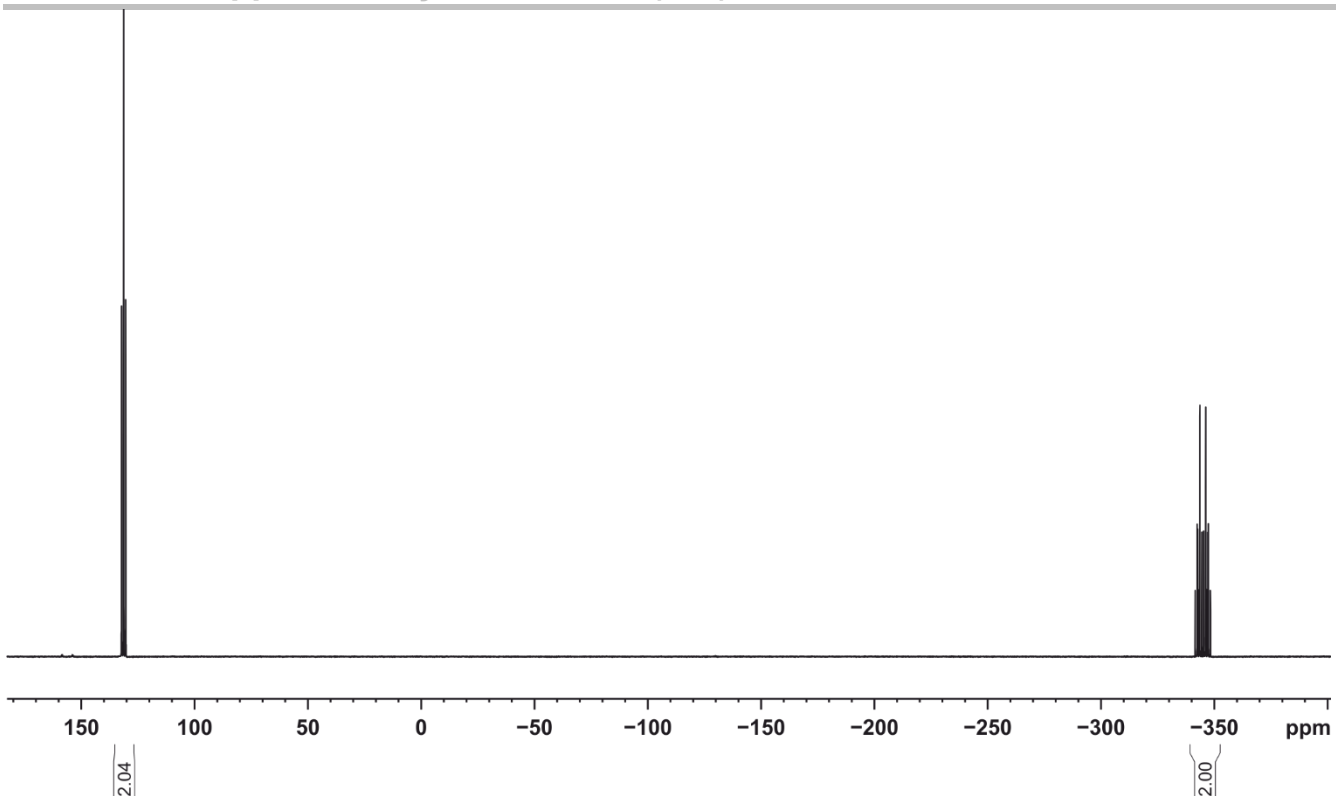

Figure S2. $^{31}P\{^1H\}$ NMR spectrum (161.98 MHz, 300 K, C_6D_6) of [LSi(η^2-P_4)].

2.2 Synthesis of [(IDipp)Ni{(μ-$\eta^{2:2}$-P_4)SiL}$_2$] (1a)

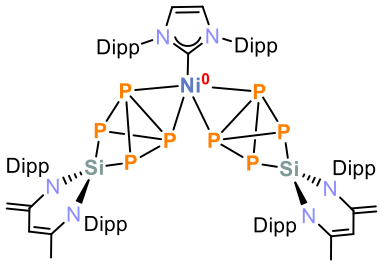

A yellow solution of [(IDipp)Ni(η^2-H_2C=CHSiMe_3)$_2$] (286 mg , 0.44 mmol, 1.0 equiv.) in 10 mL toluene was added to a pale-yellow solution of [LSi(η^2-P_4)] (500 mg, 0.88 mmol, 2.0 equiv.) in 20 mL toluene at −50 °C. The reaction mixture was stirred for 18 h. Upon warming to room temperature, the color changed from yellow to burgundy. Volatiles were removed in *vacuo*, and the resulting violet solid was redissolved in toluene and filtered through a glass frit (pore size P4). The filtrate was concentrated in *vacuo* and stored at −30 °C. Storage for 2 days resulted in the precipitation of **1a** as a violet, microcrystalline powder. According to the ^{1}H NMR spectrum the isolated product contains 1.7 toluene solvate molecules per formula unit after drying in *vacuo* (10^{-3} mbar) at 60 °C for 3 hours. Crystals suitable for single crystal X-ray diffraction analysis were obtained by slow diffusion of *n*-hexane into a concentrated toluene solution of **1a**.

Yield: 377 mg (50%).

^{1}H NMR (400.13 MHz, 300 K, C_6D_6): δ / ppm = 0.90 (d, $^3J_{HH}$ = 7 Hz, 12 H, Dipp: CH*Me$_2$*), 1.04 (d, $^3J_{HH}$ = 7 Hz, 12 H, Dipp-IDipp: CH*Me$_2$*), 1.23 (d, $^3J_{HH}$ = 7 Hz, 12 H, Dipp: CH*Me$_2$*), 1.44 (s, 6 H, L: NC*Me*), 1.44 (d, $^3J_{HH}$ = 7 Hz, 12 H, Dipp: CH*Me$_2$*), 1.51 (d, $^3J_{HH}$ = 7 Hz, 12 H, Dipp: CH*Me$_2$*), 1.53 (d, $^3J_{HH}$ = 7 Hz, 12 H, Dipp: CH*Me$_2$*), 2.95 (sept, $^3J_{HH}$ = 7 Hz, 4 H, Dipp-IDipp: C*H*Me$_2$), 3.25 (s, 2 H, L: NCC*H$_2$*), 3.67 (sept, $^3J_{HH}$ = 7 Hz, 8 H, Dipp: C*H*Me$_2$), 3.89 (s, 2 H, L: NCC*H$_2$*), 5.17 (s, 2 H, L: γ-C*H*), 6.43 (s, 2 H, IDipp: *H*C=C*H*), 6.82 (s, 4 H, IDipp: Ar-*H*), 7.22-7.47 (m, 12 H, Dipp: 2,6-*i*Pr$_2$C$_6$*H$_3$*).

$^{13}C\{^1H\}$ NMR (125.75 MHz, 300 K, C_6D_6): δ / ppm = 21.9 (L: NC*Me*), 24.10 (Dipp: CH*Me$_2$*), 28.8 (Dipp: CH*Me$_2$*), 25.3 (Dipp: CH*Me$_2$*), 25.4 (Dipp: CH*Me$_2$*), 25.8 (Dipp: CH*Me$_2$*), 27.3 (Dipp: CH*Me$_2$*), 28.0 (Dipp: *C*HMe$_2$), 28.8 (Dipp: *C*HMe$_2$), 29.2 (Dipp: *C*HMe$_2$), 86.6 (L: NC*C*H$_2$), 103.4 (L: γ-*C*H), 122.9 (IDipp: H*C*=*C*H),

123.9 (Dipp, *C*H), 124.6 (Dipp, *C*H), 124.7 (Dipp, *C*H), 125.3 (Dipp, *C*H), 128.2 (Dipp, *C*H), 129.0 (Dipp, *C*H), 129.5 (Dipp, *C*H), 136.6 (Dipp), 137.2 (Dipp), 137.5 (Dipp), 140.2 (L: N*C*Me), 145.4 (Dipp), 147.8 (L: N*C*CH_2), 148.0 (Dipp), 148.4 (Dipp). The signal of the quaternary carbon atom of the IDipp ligand could not be detected in the $^{13}C\{^1H\}$ NMR spectrum.

$^{31}P\{^1H\}$ NMR (161.98 MHz, 300 K, C_6D_6): δ / ppm = –234.3 (br, 4 P), 190.6 (br, 4 P).

^{29}Si NMR (99.36 MHz, 300 K, C_6D_6): δ / ppm = –50.5 (br).

Elemental analysis calcd. for $C_{85}H_{116}N_6NiP_8Si_2 \cdot 1.7\ C_7H_8$ (Mw = 1741.20 g·mol^{-1}): C 66.84, H 7.50, N 4.83; found C 67.20, H 7.46, N 4.80.

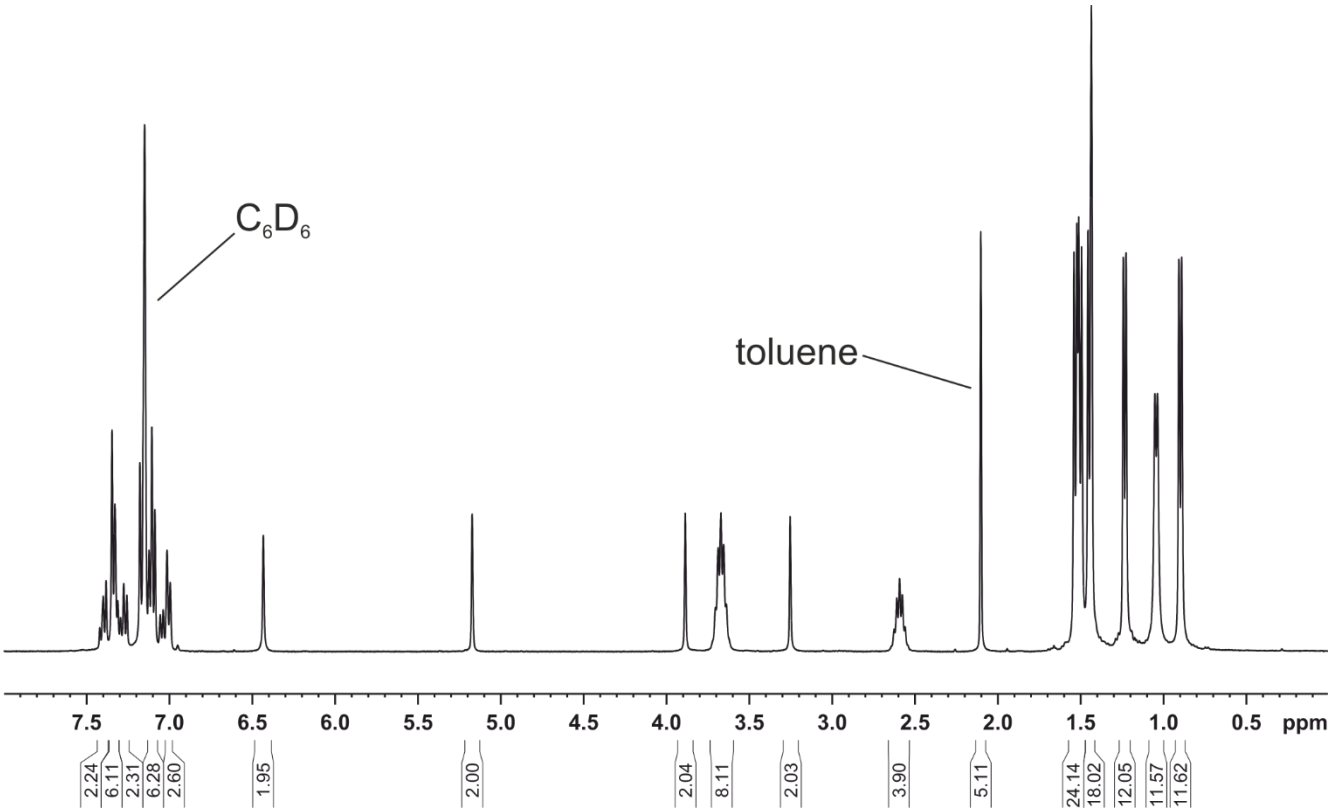

Figure S3. ^1H NMR spectrum (400 MHz, 300 K, C_6D_6) of [(IDipp)Ni{(μ-η$^{2:2}$-P_4)SiL}$_2$] (**1a**).

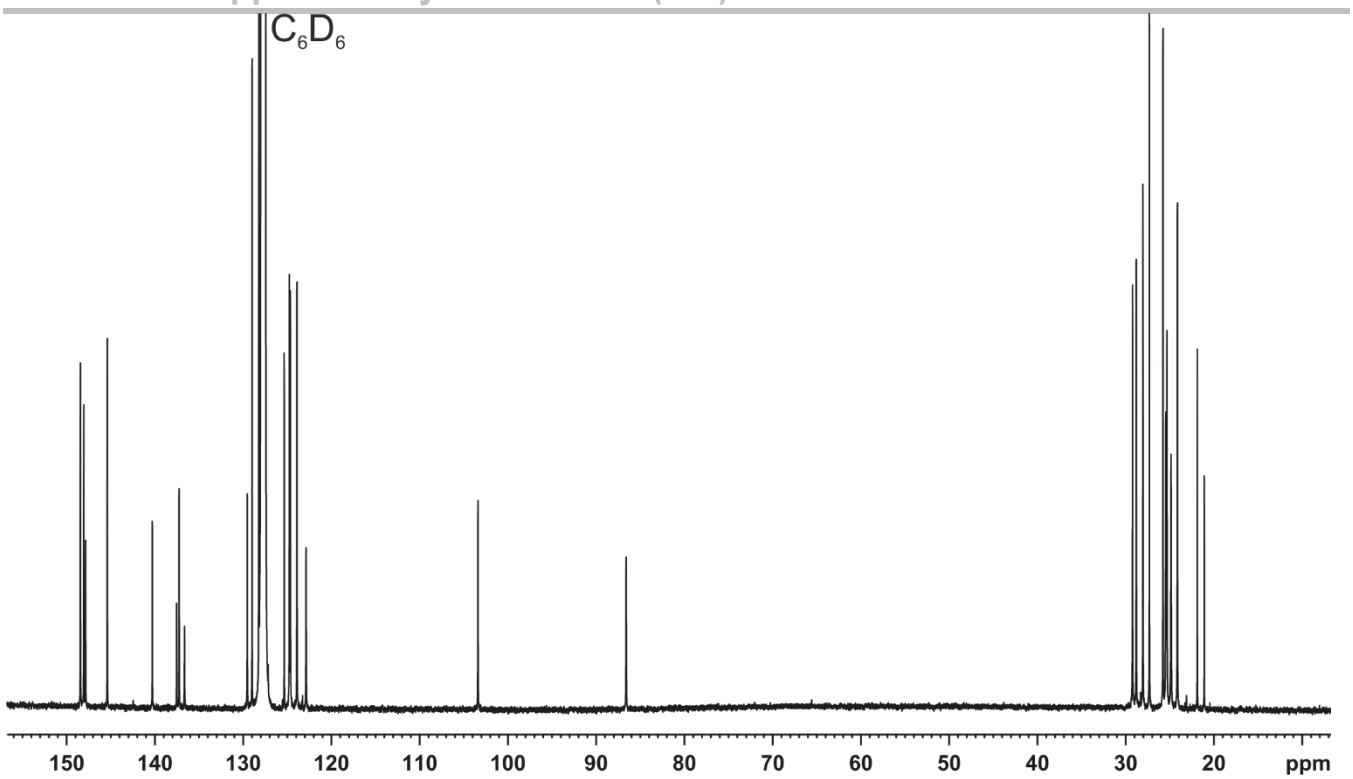

Figure S4. $^{13}C\{^{1}H\}$ NMR spectrum (125.75 MHz, 300 K, C_6D_6) of [(IDipp)Ni{(μ-η$^{2:2}$-P_4)SiL}$_2$] (**1a**).

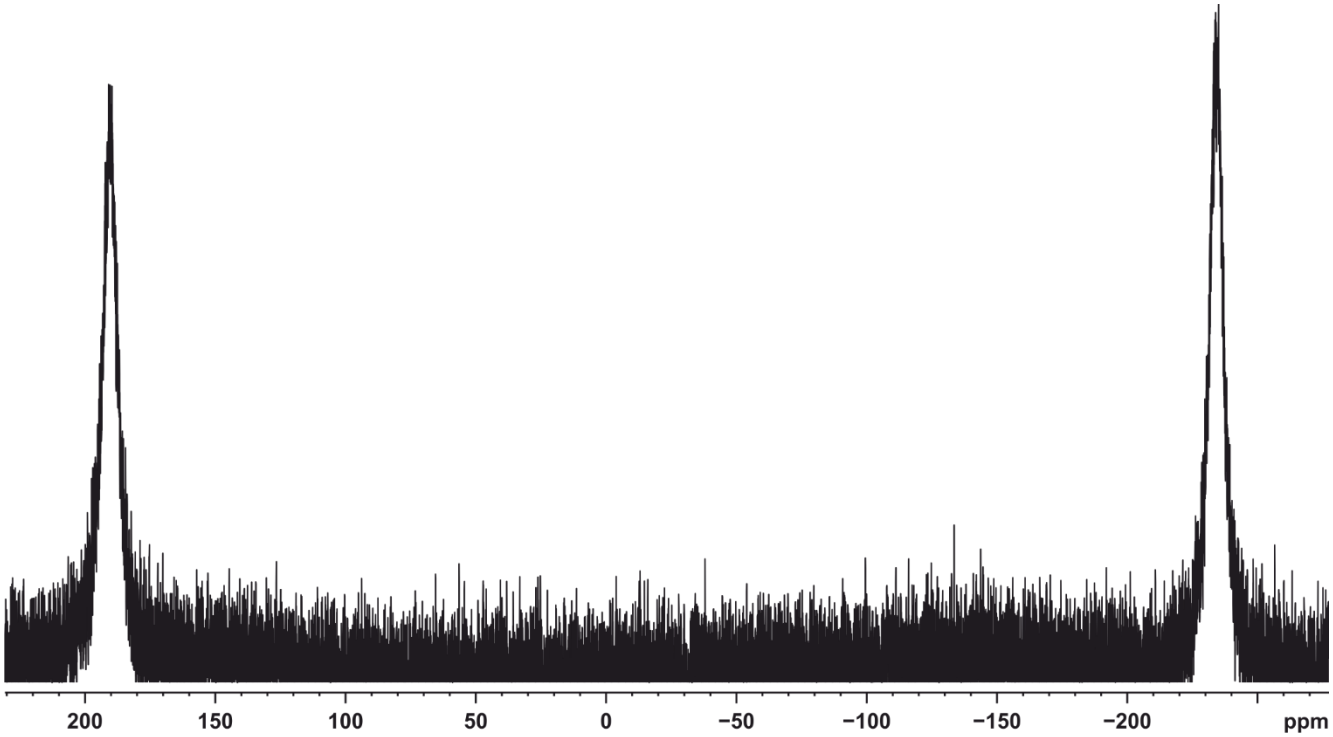

Figure S5. $^{31}P\{^{1}H\}$ NMR spectrum (161.98 MHz, 300 K, C_6D_6) of [(IDipp)Ni{(μ-η$^{2:2}$-P_4)SiL}$_2$] (**1a**).

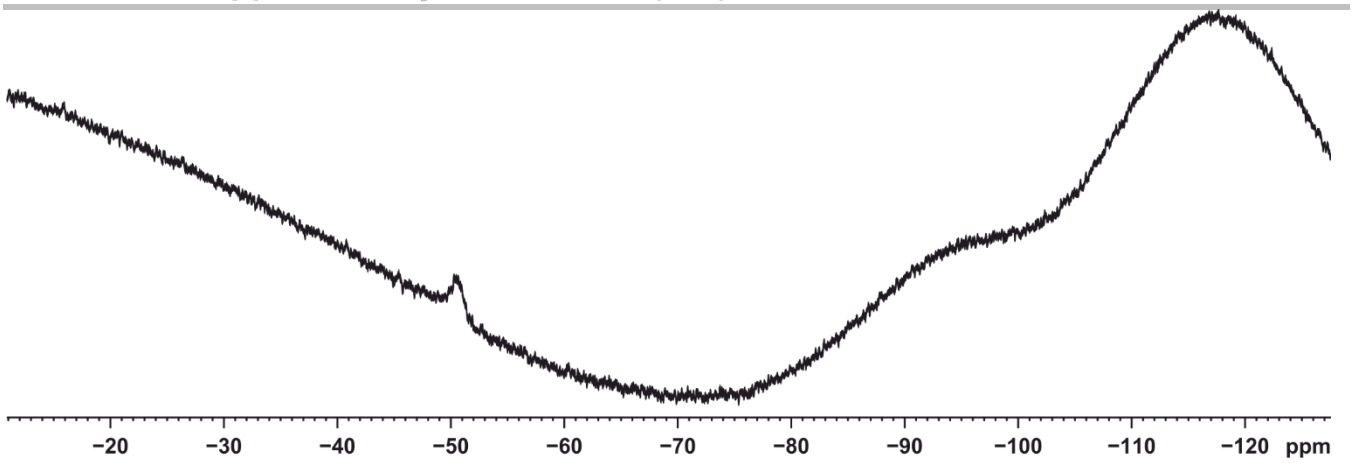

Figure S6. ^{29}Si NMR spectrum (99.36 MHz, 300 K, C_6D_6) of [(IDipp)Ni{(μ-η$^{2:2}$-P_4)SiL}$_2$] (**1a**).

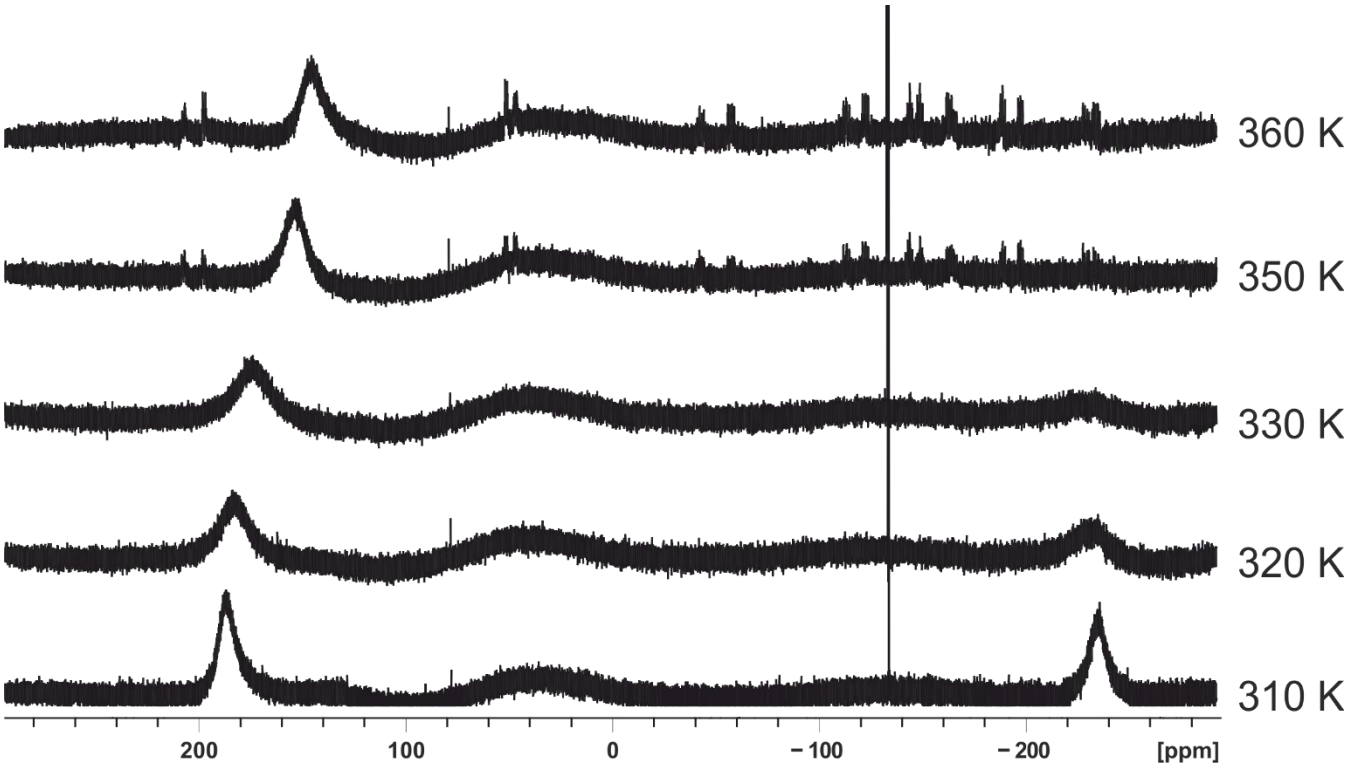

Figure S7. VT ^{31}P{^{1}H} NMR spectra of [(IDipp)Ni{(μ-η$^{2:2}$-P_4)SiL}$_2$] (**1a**) in tol-d_8. The sample used for the VT ^{31}P{^{1}H} NMR experiments shows a minor impurity which resonates at –153.0 ppm. Upon heating to 350 K complex **1a** thermolysis to form cluster compound **3**.

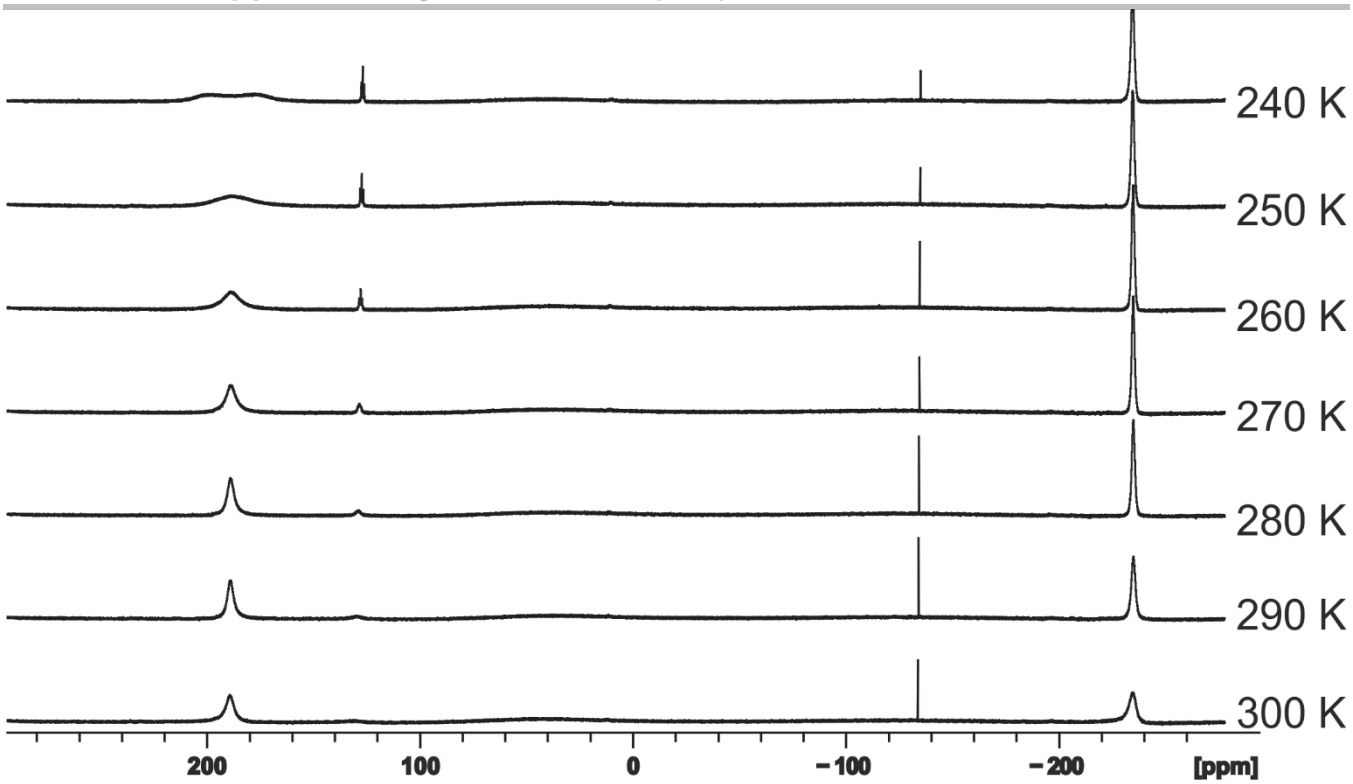

Figure S8. VT $^{31}P\{^{1}H\}$ NMR spectra of [(IDipp)Ni{(μ-$\eta^{2:2}$-P_4)SiL}$_2$] (**1a**) in tol-d_8. The sample used for the VT $^{31}P\{^{1}H\}$ NMR experiments shows some minor impurities which resonate at –153.0 ppm as well as small amounts of [LSi(η^2-P_4)].

2.3 Synthesis of [(IMes)Ni{(μ-η$^{2:2}$-P$_4$)SiL}$_2$] (1b)

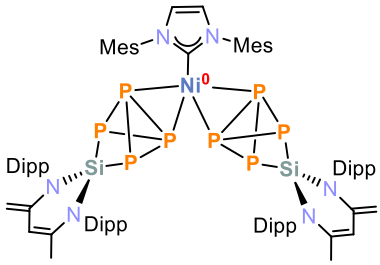

A yellow solution of [(IMes)Ni(η^2-H$_2$C=CHSiMe$_3$)$_2$] (0.91 g, 1.60 mmol, 1.0 equiv.) in 20 mL toluene was added to a pale yellow solution of [LSi(η^2-P$_4$)] (1.81 g, 3.20 mmol, 2.0 equiv.) in 30 mL toluene at −50 °C. The reaction mixture was stirred for 18 h. Upon warming to room temperature, the color changed from yellow to burgundy red. Volatiles were removed in *vacuo*, and the resulting violet solid was redissolved in toluene and filtered through a glass frit (pore size P4). The filtrate was concentrated in *vacuo* and stored at −30 °C. After 2 day, a violet microcrystalline precipitate of **1b** had formed. According to the ^{1}H NMR spectrum, the isolated product contains 0.21 toluene solvate molecules per formula unit after drying in *vacuo* (10^{-3} mbar) over 5 hours. Crystals suitable for single crystal X-ray diffraction analysis were obtained by slow evaporation of a concentrated solution of **1b** dissolved in *n*-hexane.

Yield: 620 mg (26%).

^{1}H NMR (400.13 MHz, 300 K, C$_6$D$_6$): δ / ppm = 1.19 (d, $^3J_{HH}$ = 7 Hz, 12 H, Dipp: CH*Me$_2$*), 1.44 (d, $^3J_{HH}$ = 7 Hz, 12 H, Dipp: CH*Me$_2$*), 1.48 (s, 6 H, L: NC*Me*), 1.52 (d, $^3J_{HH}$ = 7 Hz, 24 H, Dipp: CH*Me$_2$*), 1.75 (s, 12 H, IMes: *o*-Ar-*Me*), 2.43 (s, 6 H, IMes: *p*-Ar-*Me*), 3.28 (s, 2 H, L: NCC*H$_2$*), 3.60 (sept, $^3J_{HH}$ = 7 Hz, 4 H, Dipp: C*H*Me$_2$), 3.66 (sept, $^3J_{HH}$ = 7 Hz, 4 H, Dipp: C*H*Me$_2$), 3.91 (s, 2 H, L: NCC*H$_2$*), 5.21 (s, 2 H, L: γ-C*H*), 6.12 (s, 2 H, IMes: *H*C=C*H*), 6.82 (s, 4 H, IMes: Ar-*H*), 7.22-7.47 (m, 12 H, Dipp: 2,6-*i*Pr$_2$C$_6$*H$_3$*).

^{13}C{^{1}H} NMR (100.61 MHz, 300 K, C$_6$D$_6$): δ / ppm = 19.1 (IMes: *o*-C$_6$H$_2$*Me$_3$*), 21.3 (IMes: *p*-C$_6$H$_2$*Me$_3$*), 22.1 (L: NC*Me*), 24.8 (Dipp: CH*Me$_2$*), 25.3 (Dipp: CH*Me$_2$*), 26.0 (Dipp: CH*Me$_2$*), 27.7 (Dipp: CH*Me$_2$*), 29.0 (Dipp: *C*HMe$_2$), 29.4 (Dipp: *C*HMe$_2$), 86.6 (L: NC*C*H$_2$), 103.2 (L: γ-*C*H), 121.5 (IMes: H*C*=*C*H), 124.6 (Ar: *C*H), 124.8 (Ar: *C*H), 129.2 (Ar: *C*H), 136.1 (Ar), 136.7 (Ar), 137.4 (Ar), 137.5 (Ar), 137.7 (Ar), 140.7 (L: N*C*Me), 148.3 (L: N*C*CH$_2$), 148.7 (Ar), 149.2 (Ar). The quaternary carbon atom of the IMes ligand could not be detected in the ^{13}C{^{1}H} NMR spectrum.

^{31}P{^{1}H} NMR (161.98 MHz, 300 K, C$_6$D$_6$): δ / ppm = –236.4 (m, 4 P), 194.2 (m, 4 P).

^{29}Si NMR (99.36 MHz, 300 K, THF-*d$_8$*): δ / ppm = –52.1 (broad pseudo-triplet).

Elemental analysis calcd. for C$_{79}$H$_{104}$N$_6$NiP$_8$Si$_2$ · 0.21 C$_7$H$_8$ (Mw = 1519.73 g·mol^{-1}): C 63.43, H 7.00, N 5.56; found C 63.60, H 7.01, N 5.53.

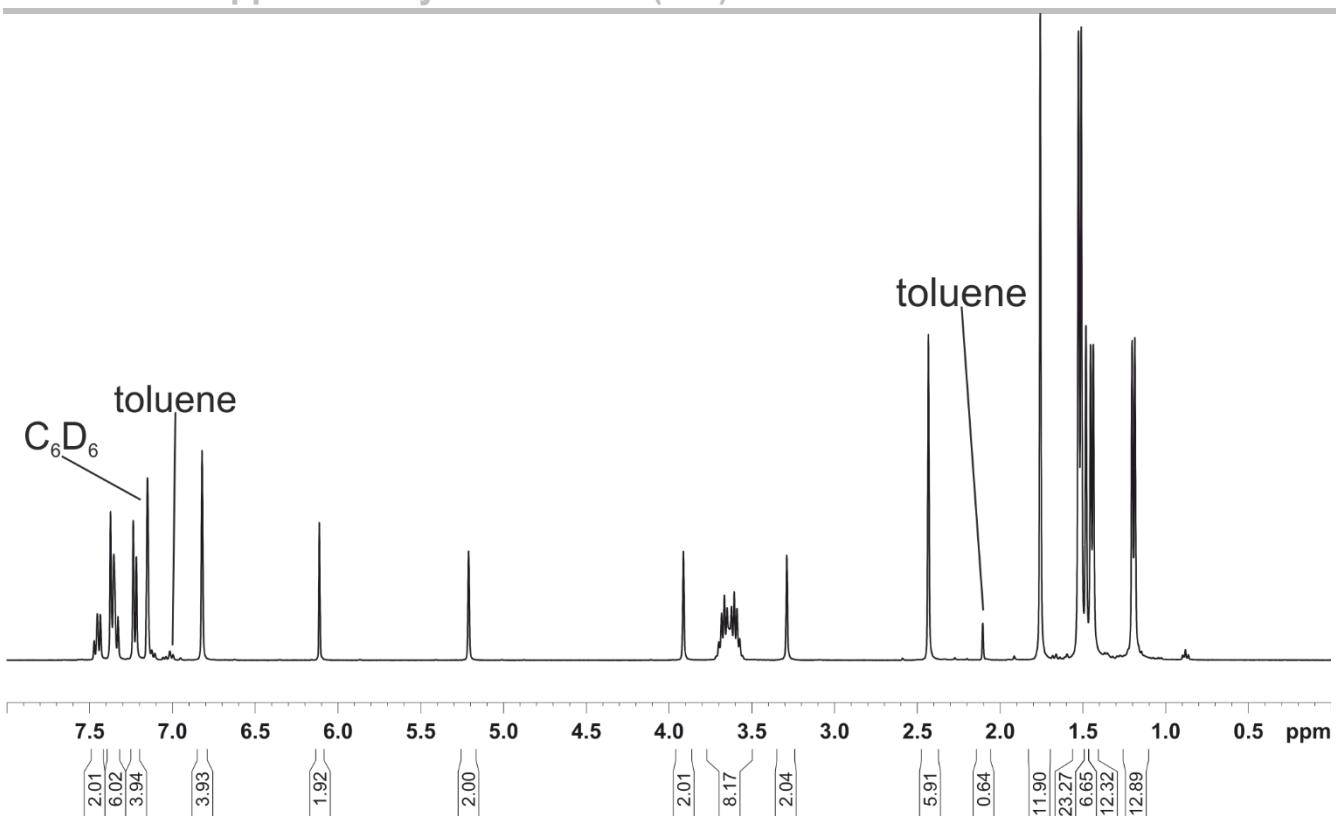

Figure S9. ^{1}H NMR spectrum (400 MHz, 300 K, C_6D_6) of [(IMes)Ni{(μ-η$^{2:2}$-P_4)SiL}$_2$] (**1b**).

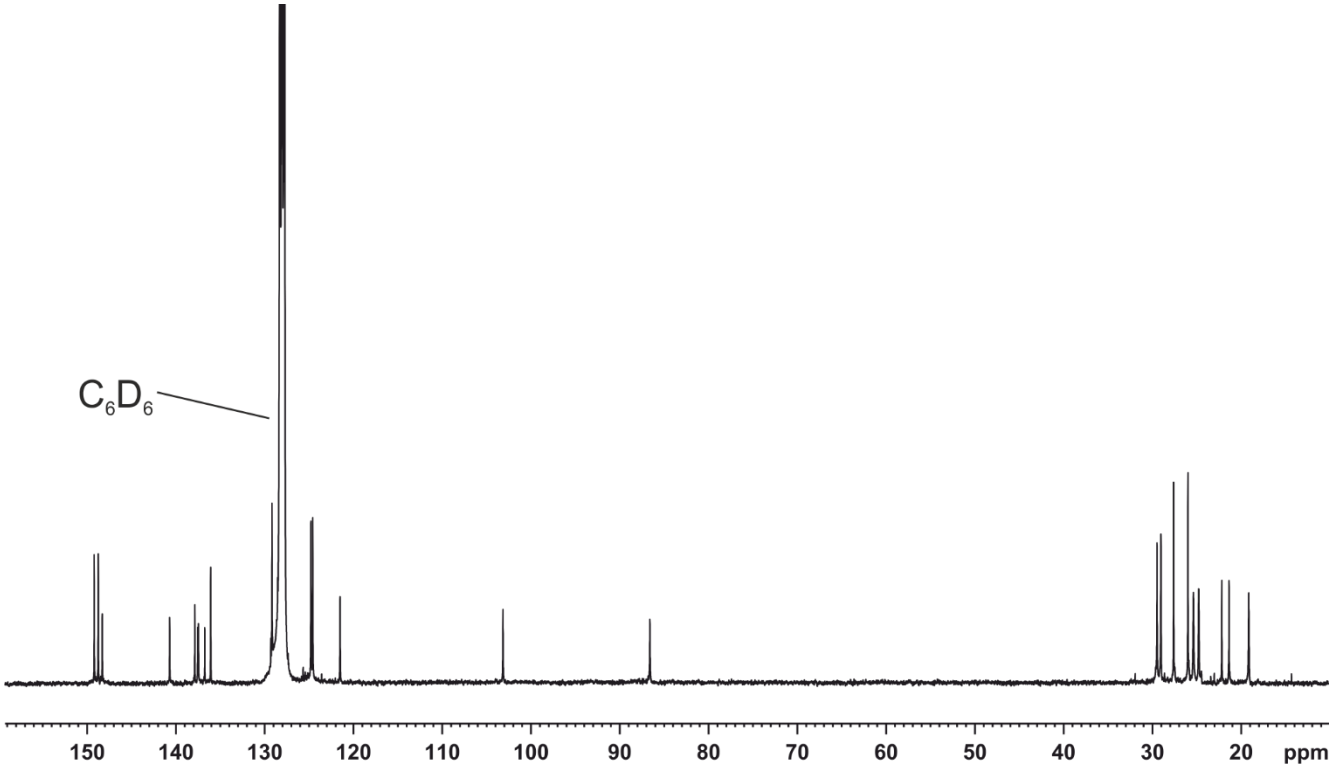

Figure S10. ^{13}C{^{1}H} NMR spectrum (100.61 MHz, 300 K, C_6D_6) of [(IMes)Ni{(μ-η$^{2:2}$-P_4)SiL}$_2$] (**1b**).

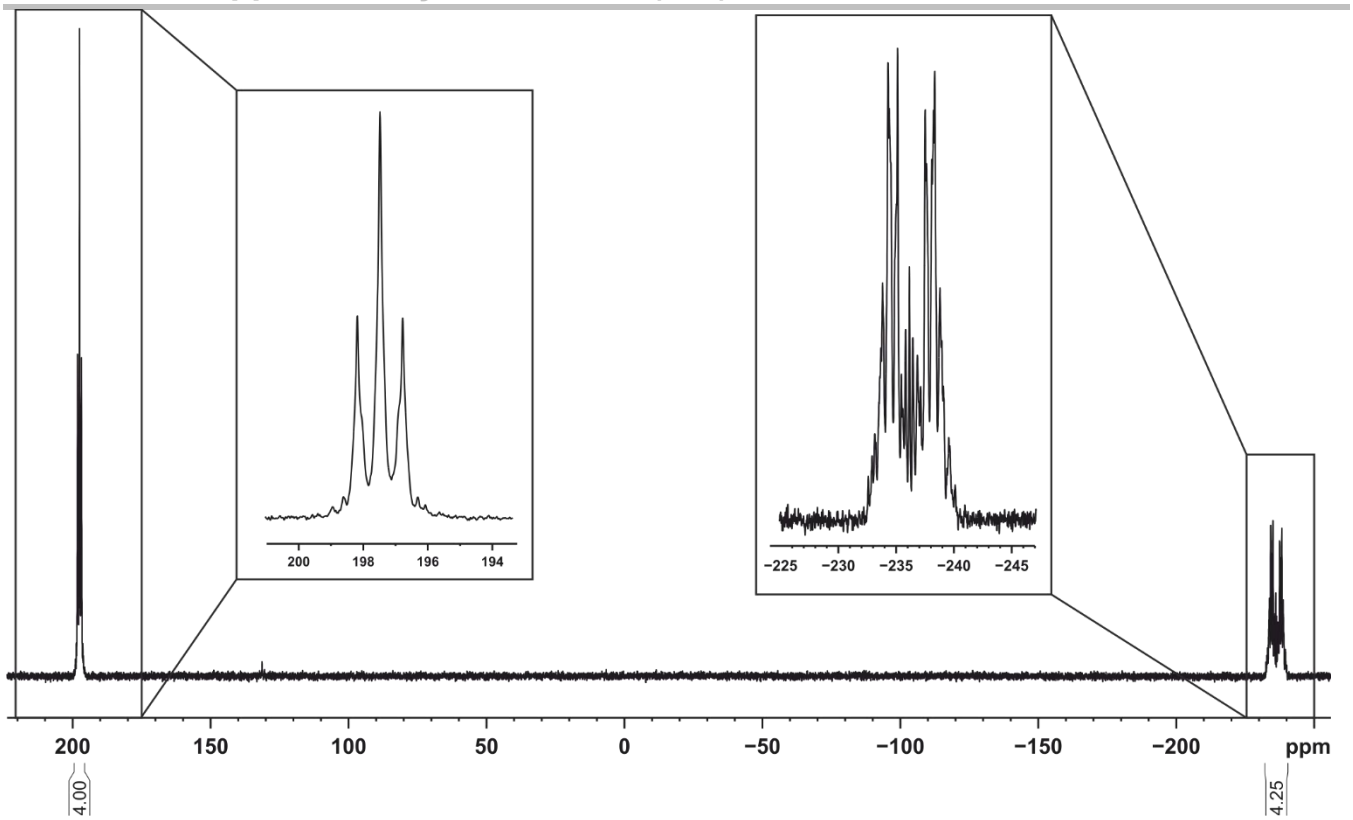

Figure S11. $^{31}P\{^{1}H\}$ NMR spectrum (161.98 MHz, 300 K, C_6D_6) of [(IMes)Ni{(μ-η$^{2:2}$-P_4)SiL}$_2$] (**1b**).

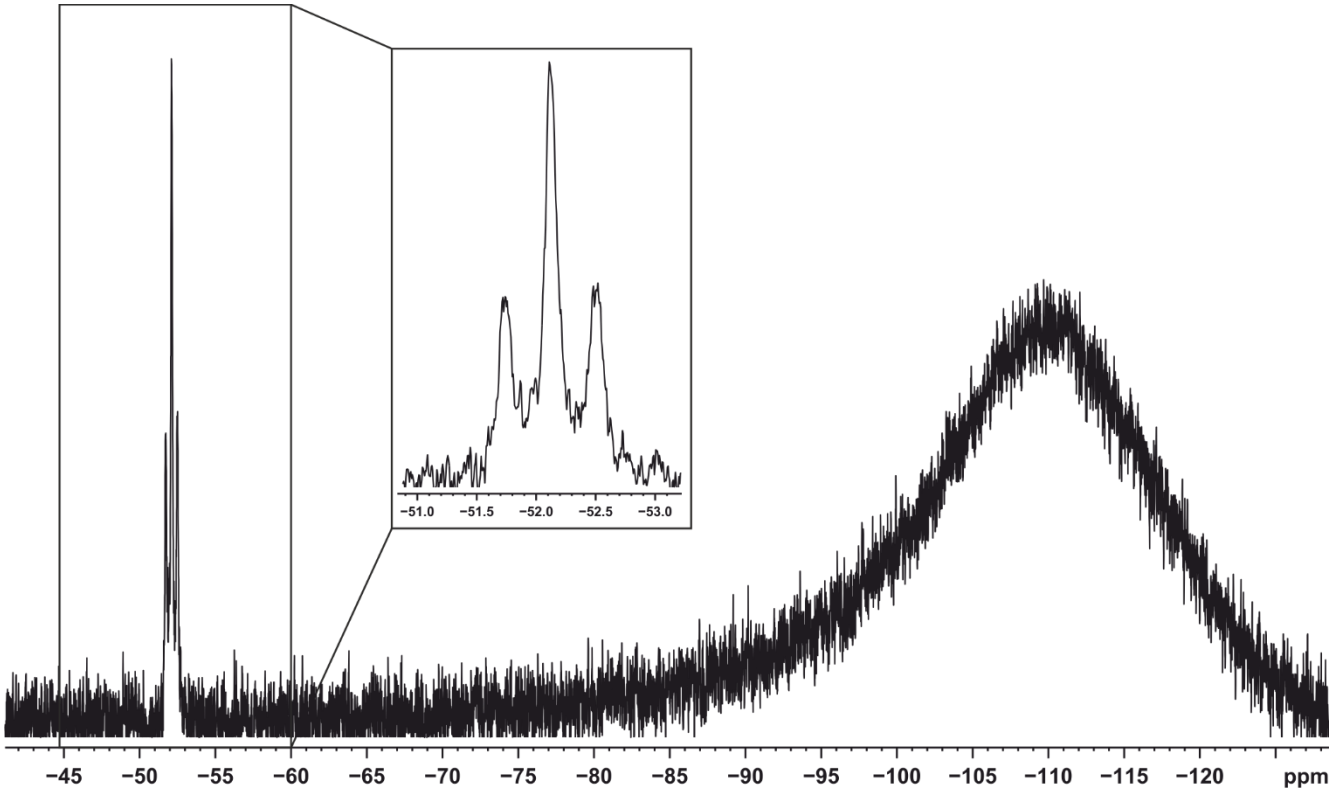

Figure S12. ^{29}Si NMR spectrum (99.36 MHz, 300 K, THF-d_8) of [(IMes)Ni{(μ-η$^{2:2}$-P_4)SiL}$_2$] (**1b**).

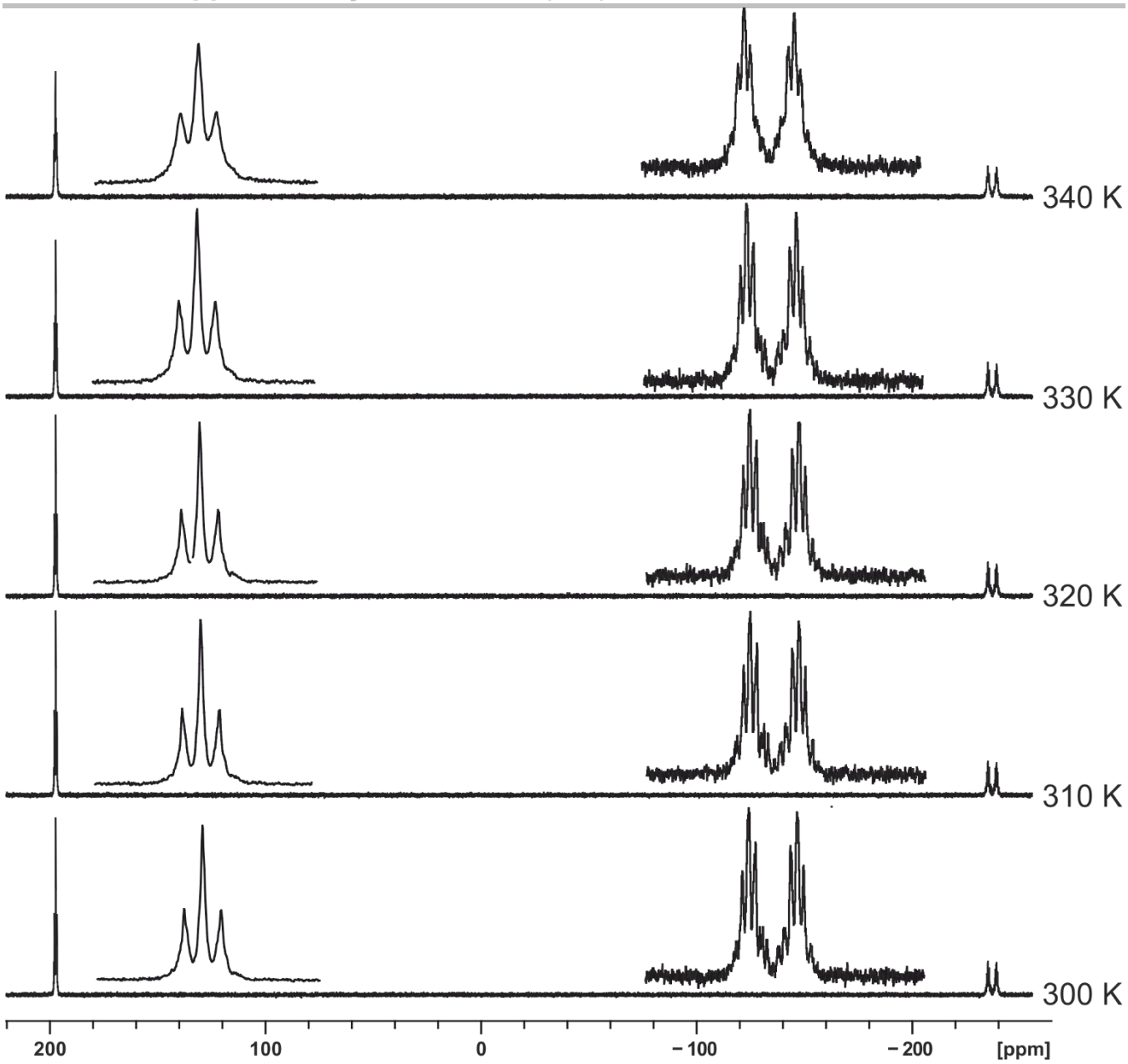

Figure S13. VT $^{31}P\{^{1}H\}$ NMR spectra of [(IMes)Ni{(μ-$\eta^{2:2}$-P_4)SiL}$_2$] (**1b**) in tol-d_8.

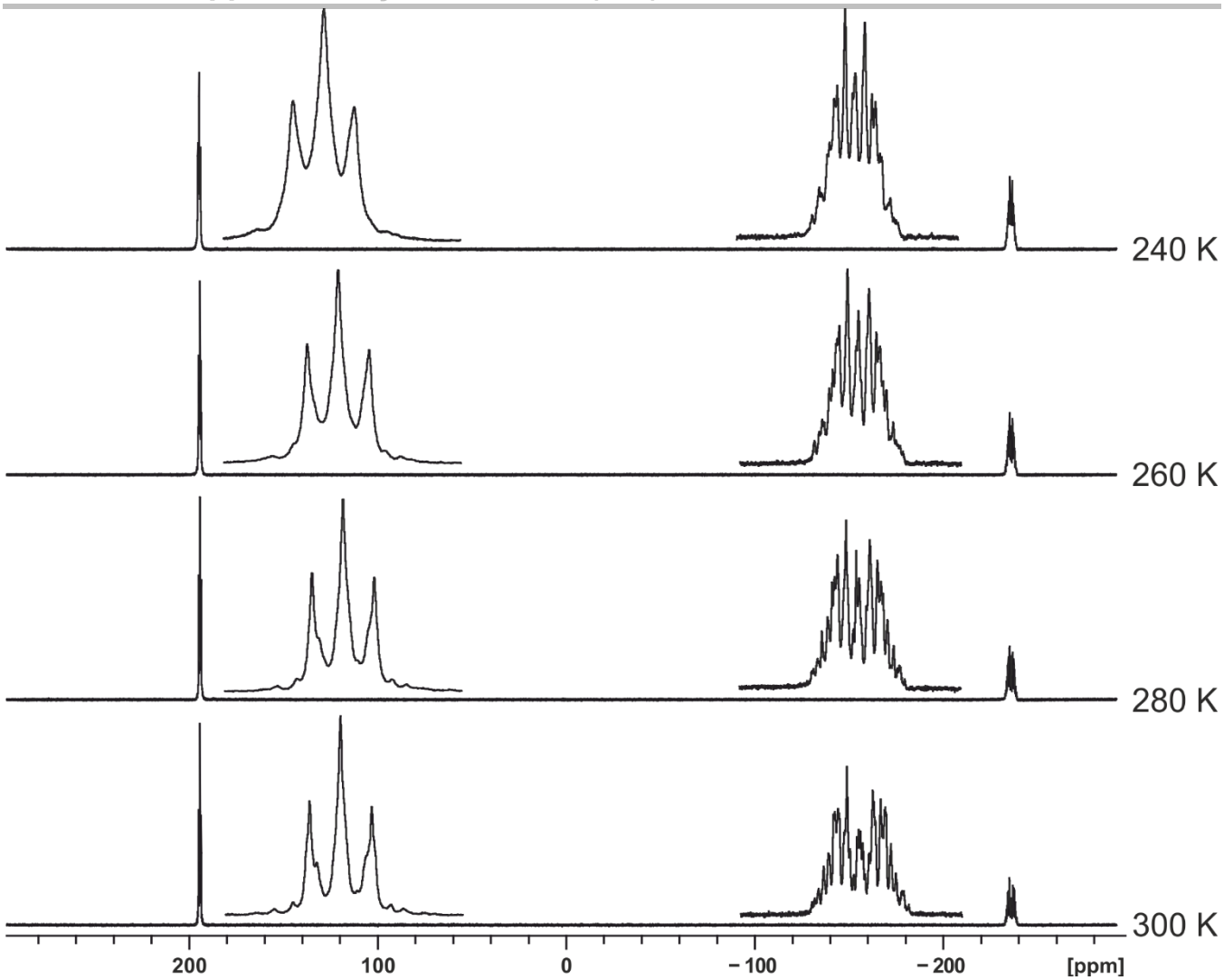

Figure S14. VT $^{31}P\{^{1}H\}$ NMR spectra of [(IMes)Ni{(μ-$\eta^{2:2}$-P_4)SiL}$_2$] (**1b**) in THF-d_8.

2.4 Synthesis of [(IDipp)Ni(μ-η$^{2:2}$-P$_4$)SiL] (2)

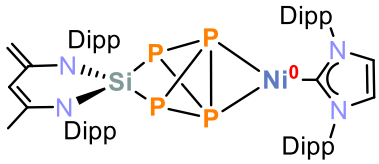

A pale-yellow solution of [LSi(η^2-P$_4$)] (432.6 mg, 0.77 mmol, 1.0 equiv.) in toluene (15 ml) was added dropwise to a yellow solution of [(IDipp)Ni(η^2-H$_2$C=CHSiMe$_3$)$_2$] (500 mg, 0.77 mmol, 1.0 equiv.) in toluene (15 ml) at room temperature. The reaction mixture was stirred for 18 hours at room temperature, whereupon the color changed to brown. Volatiles were removed in *vacuo* and the brown residue was extracted with *n*-hexane (60 mL) using a glass frit (pore size P4). The filtrate was concentrated to 25 mL. Storage at −30 °C for 2 days gave **2** as an analytically pure, microcrystalline powder. According to the ^{1}H NMR spectrum the isolated product contains 0.36 *n*-hexane solvate molecules per formula unit after drying in *vacuo* (10^{-3} mbar) over period of 3 hours. Crystals suitable for single crystal X-ray diffraction analysis were obtained by slow evaporation of a concentrated solution of **2** dissolved in *n*-hexane.
N.B. Complex **2** is unstable in solution and converts slowly into compound **3** at room temperature.

Yield: 240 mg (33%).

^{1}H NMR (400.13 MHz, 300 K, C$_6$D$_6$): δ / ppm = 1.02 (d, $^3J_{HH}$ = 7 Hz, 12 H, Dipp: CH*Me$_2$*), 1.14 (d, $^3J_{HH}$ = 7 Hz, 6 H, Dipp: CH*Me$_2$*), 1.42 (d, $^3J_{HH}$ = 7 Hz, 18 H, Dipp: CH*Me$_2$*), 1.49 (m, 12 H, Dipp: CH*Me$_2$* and 3 H L: NC*Me*), 2.57 (sept, $^3J_{HH}$ = 7 Hz, 4 H, Dipp-IDipp: C*H*Me$_2$), 3.25 (s, 1 H, L: NCC*H$_2$*), 3.73 (sept, $^3J_{HH}$ = 7 Hz, 2 H, Dipp: C*H*Me$_2$), 3.79 (sept, $^3J_{HH}$ = 7 Hz, 2 H, Dipp: C*H*Me$_2$), 3.89 (s, 1 H, L: NCC*H$_2$*), 5.26 (s, 1 H, L: γ-C*H*), 6.16 (s, 2 H, IDipp: *H*C=C*H*), 6.98-7.35 (m, 12 H, Dipp: 2,6-*i*Pr$_2$C$_6$*H$_3$*).

^{13}C{^{1}H} NMR (100.61 MHz, 300 K, C$_6$D$_6$): δ / ppm = 21.8 (L: NC*Me*), 23.9 (Dipp: CH*Me$_2$*), 24.6 (Dipp: CH*Me$_2$*), 25.6 (Dipp: CH*Me$_2$*), 27.2 (Dipp: CH*Me$_2$*), 28.5 (IDipp: *C*HMe$_2$), 28.6 (L: *C*HMe$_2$), 29.0 (L: *C*HMe$_2$), 85.6 (L: NC*C*H$_2$), 102.8 (L: γ-*C*H), 121.6 (IDipp: H*C*=*C*H), 123.7 (Dipp, *C*H), 124.2 (Dipp, *C*H),124.4 (Dipp, *C*H), 130.0 (Dipp, *C*H), 135.1 (Dipp), 137.3 (Dipp), 137.6 (Dipp), 140.3 (L: N*C*Me), 145.3 (Dipp), 148.1 (L: N*C*CH$_2$), 148.5 (Dipp). The quaternary carbon atom of the IDipp ligand could not be detected in the ^{13}C{^{1}H} NMR spectrum.

^{31}P{^{1}H} NMR (161.98 MHz, 300 K, C$_6$D$_6$): ABX$_2$ spin system; δ / ppm ABX$_2$ δ(P$_A$) = −155.1 (dt, ^1J(P$_A$,P$_X$) = −114.2 Hz, ^1J(P$_A$,P$_B$) = −25.6 Hz), δ(P$_B$) = −138.0 (dt, ^1J(P$_B$,P$_X$) = −114.1 Hz, ^1J(P$_A$,P$_B$) = −25.6 Hz), δ(P$_X$) = 147.3 (dd, ^1J(P$_X$,P$_A$) = −114.2 Hz, ^1J(P$_X$,P$_B$) = −114.1 Hz).

^{29}Si NMR (99.36 MHz, 300 K, C$_6$D$_6$): δ / ppm = −37.1 (br).

Elemental analysis calcd. for C$_{56}$H$_{76}$N$_4$NiP$_4$Si · 0.36 C$_6$H$_{14}$ (Mw = 1046.95 g·mol^{-1}): C 66.72, H 7.80, N 5.35; found C 66.91, H 7.40, N 5.38.

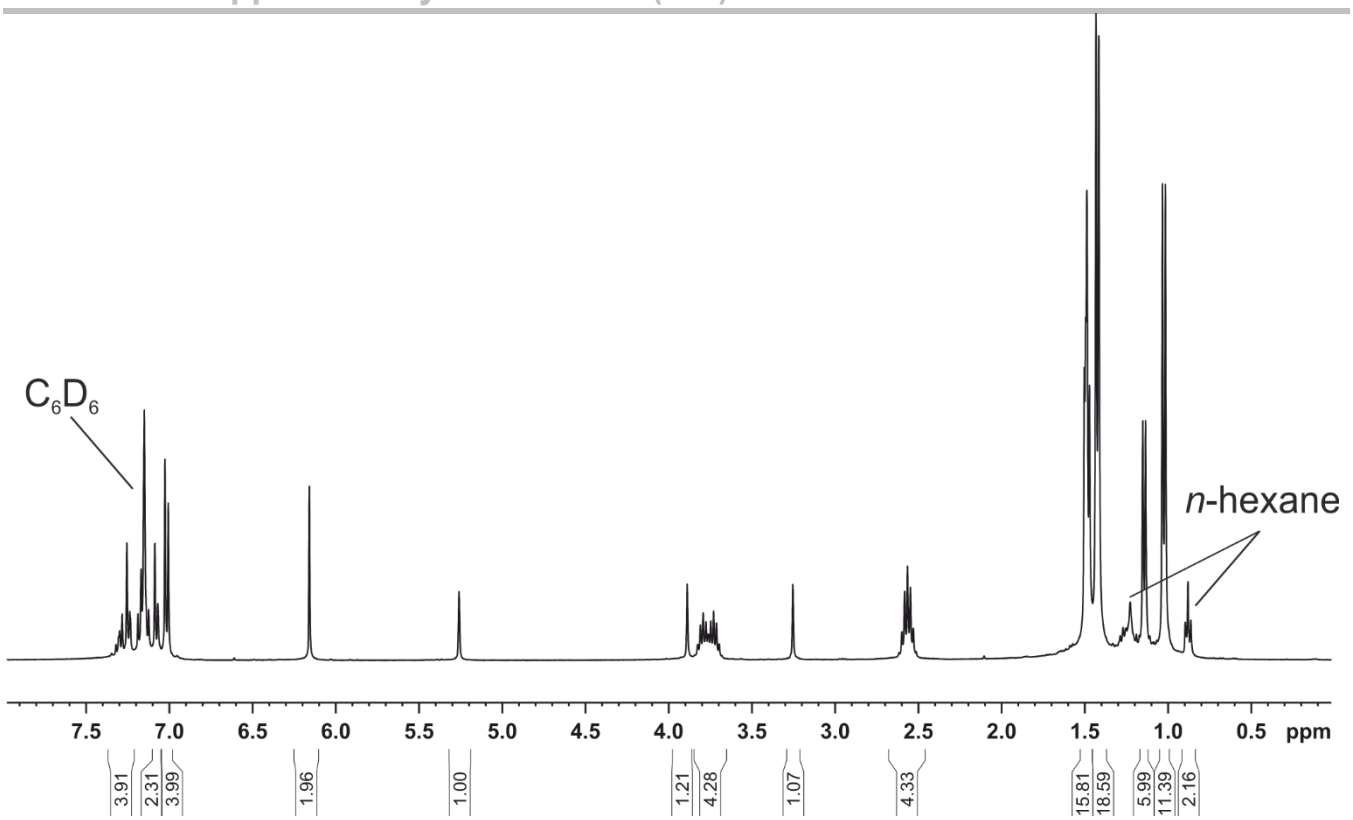

Figure S15. ^{1}H NMR spectrum (400 MHz, 300 K, C_6D_6) of [(IDipp)Ni(μ-η$^{2:2}$-P_4)SiL] (**2**).

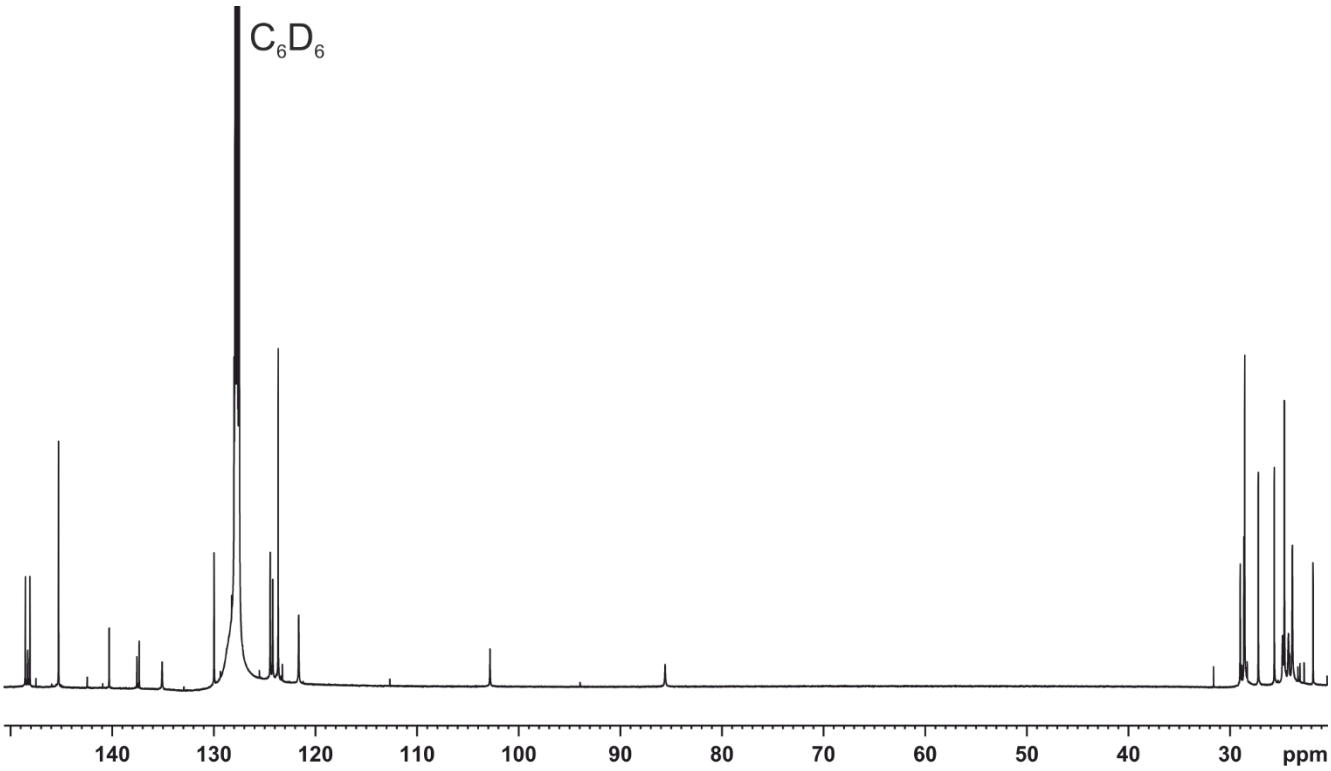

Figure S16. ^{13}C{^{1}H} NMR spectrum (125.75 MHz, 300 K, C_6D_6) of [(IDipp)Ni(μ-η$^{2:2}$-P_4)SiL] (**2**).

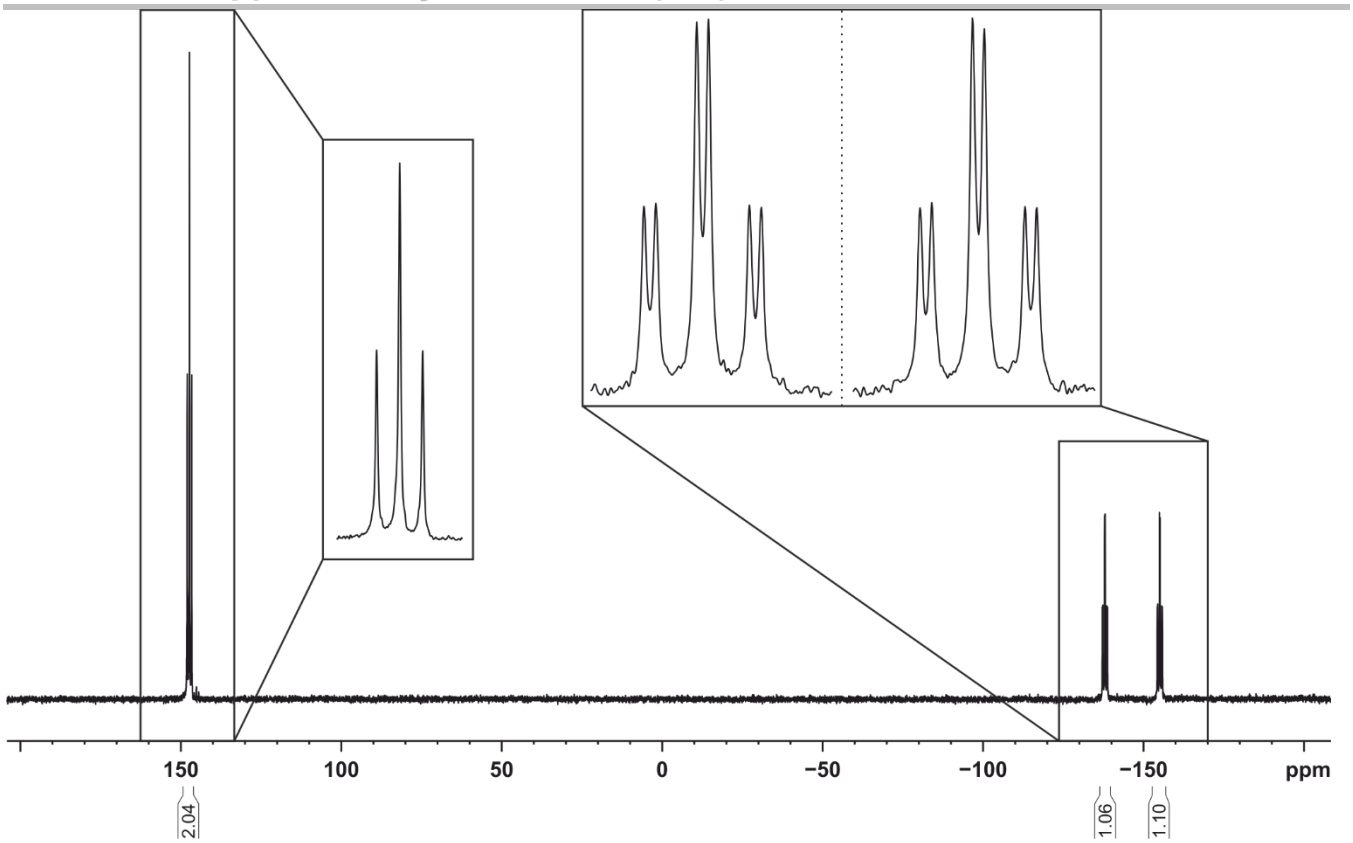

Figure S17. $^{31}P\{^{1}H\}$ NMR spectrum (161.98 MHz, 300 K, C_6D_6) of [(IDipp)Ni(μ-$\eta^{2:2}$-P_4)SiL] (**2**).

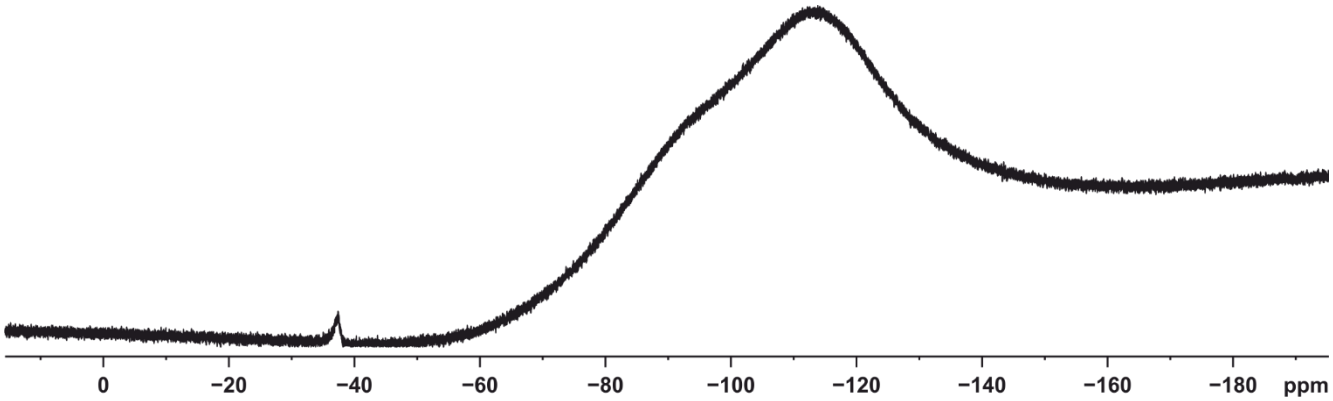

Figure S18. ^{29}Si NMR spectrum (99.36 MHz, 300 K, C_6D_6) of [(IDipp)Ni(μ-$\eta^{2:2}$-P_4)SiL] (**2**).

2.5 Synthesis of [(IDipp)Ni$_2$P$_8$(SiL)$_2$] (3)

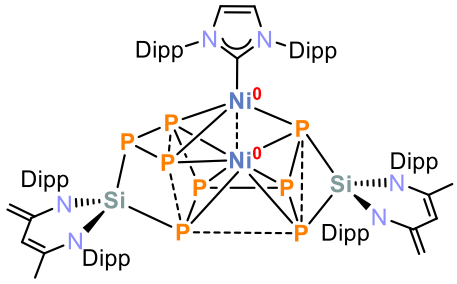

A pale-yellow solution of [LSi(η^2-P$_4$)] (217.2 mg, 0.38 mmol, 1.0 equiv.) in toluene (15 ml) was added dropwise to a yellow solution of [(IDipp)Ni(η^2-H$_2$C=CHSiMe$_3$)$_2$] (247.8 mg, 0.38 mmol, 1.0 equiv.) in toluene (15 ml) at room temperature. The reaction mixture was stirred for 18 hours at 60 °C, whereupon the color changed to brown. Volatiles were removed in *vacuo* and the remaining brown solid was transferred to a sublimation apparatus. Free carbene IDipp, was removed by vacuum sublimation (95 °C, 1·10^{-5} mbar). The residual solid was redissolved in toluene (60 mL) and filtered through a glass frit (pore size P4). The solution was concentrated to a volume of 15 mL. Layering the concentrated toluene solution with *n*-hexane gave brownish crystals of **3** after one week. Crystals suitable for single crystal X-ray diffraction analysis were obtained by slow evaporation of a concentrated *n*-hexane solution of **3**.

Yield: 240 mg (33%).

N.B. Two isomers (labelled A and B) were detected in the NMR spectra and by single crystal X-ray diffraction experiments. These isomers cannot be separated and are assigned via their respective integrations in the ^{1}H and ^{31}P{^{1}H} NMR spectra (major isomer: A, minor isomer: B).

^{1}H NMR (400.13 MHz, 300 K, C$_6$D$_6$): signals of isomers A and B partly overlap strongly; δ / ppm = 0.09 (m, Dipp: CH*Me$_2$*), 0.59 (d, Isomer B, Dipp: CH*Me$_2$*), 0.67 (d, Isomer B, Dipp: CH*Me$_2$*), 0.75 (d, Isomer A, Dipp: CH*Me$_2$*), 0.851–1.65 (m, Dipp: CH*Me$_2$* overlap with L: NC*Me*), 1.71 (d, Isomer B, Dipp: CH*Me$_2$*), 1.75 (d, Isomer A, Dipp: CH*Me$_2$*), 1.86 (d, Isomer A, Dipp: CH*Me$_2$*); (integrals fit to the 78 expected hydrogen atoms); 1.97 (m, Dipp: C*H*Me$_2$), 2.34 (sept, Isomer B, Dipp: C*H*Me$_2$), 2.48 (sept, Isomer A, Dipp: C*H*Me$_2$), 2.62 (m, Isomer A, Dipp: C*H*Me$_2$), 2.67 (m, Isomer B, Dipp: C*H*Me$_2$), 2.74 (sept, Isomer A, Dipp: C*H*Me$_2$), 2.85 (sept, Isomer B, Dipp: C*H*Me$_2$), 3.23 (m, Dipp: C*H*Me$_2$), 3.60 (sept, Isomer B, Dipp: C*H*Me$_2$), 3.66–3.90 (m, Dipp: C*H*Me$_2$), 4.11 (sept, Isomer A, Dipp: C*H*Me$_2$); (integrals fit to the 12 expected hydrogen atoms of the Dipp: C*H*Me$_2$ groups); 3.33 (s, Isomers A,B, L: NCC*H$_2$*), 3.37 (s, Isomer A, L: NCC*H$_2$*), 3.39 (s, Isomer B, L: NCC*H$_2$*), 3.92 (s, Isomer B, L: NCC*H$_2$*), 3.97 (s, Isomer A, L: NCC*H$_2$*), 4.00 (s, Isomer B, L: NCC*H$_2$*), 4.03 (s, Isomer A, L: NCC*H$_2$*); (integrals fit to the 4 expected hydrogen atoms of the L: NCC*H$_2$* moiety); 5.35 (s, Isomer A, L: γ-C*H*), 5.39 (s, Isomer B, L: γ-C*H*), 5.42 (s, Isomer B, L: γ-C*H*); integrals fit to the 2 expected hydrogen atoms of the L: γ-C*H* moiety); 6.34 (m, IDipp: *H*C=C*H*), 6.50 (m, IDipp: *H*C=C*H*); (integrals fit to the 2 expected hydrogen atoms of the IDipp: *H*C=C*H* backbone); 6.84–737 (m, Dipp: 2,6-*i*Pr$_2$C$_6$*H$_3$*); (integrals fit to the 18 expected hydrogen atoms of the Dipp: 2,6-*i*Pr$_2$C$_6$*H$_3$* group).

^{13}C{^{1}H} NMR (100.61 MHz, 300 K, C$_6$D$_6$): δ / ppm = 21.6, 21.7, 22.2, 22.3, 22.5, 22.5, 23.1, 23.2, 23.6, 23.7, 23.8, 23.9, 23.9, 24.3, 24.3, 24.4, 24.6, 24.7, 25.1, 25.3, 25.4, 25.4, 25.5, 25.7, 25.9, 26.0, 26.2, 26.4, 26.5, 26.6, 26.7, 26.9, 27.0, 27.1, 27.3, 27.4, 27.7, 27.8, 27.9, 28.0, 28.1, 28.1, 28.2, 28.3, 28.4, 28.7, 28.8, 28.9, 28.9, 29.0, 29.2, 29.4, 29.5 (Dipp: *C*HMe$_2$, Dipp: CH*Me$_2$*, and L: NC*Me*), 87.4, 90.6 (L: NC*C*H$_2$ Isomer B), 89.4, 90.6 (L: NC*C*H$_2$, Isomer A), 103.1, 109.4 (L: γ-*C*H, Isomer B), 106.4, 108.6 (L: γ-*C*H, Isomer A), 123.4, 123.7, 123.8, 123.9, 123.9, 124.1, 124.1, 124.2, 124.3, 124.5, 124.9, 125.0, 125.1, 128.2, 128.2, 128.3, 128.3, 129.0, 130.2, 130.3, 130.8 (Dipp, *C*H),126 (IDipp: H*C*=*C*H, Isomer B), 126.3 (IDipp: H*C*=*C*H, Isomer A), 126.5 (IDipp: H*C*=*C*H, Isomer B), 126.7 (IDipp: H*C*=*C*H, Isomer B), 140.6 (L: N*C*Me, Isomer B), 140.7 (L: N*C*Me, Isomer A), 141.6 (L: N*C*Me Isomer A), 141.8 (L: N*C*Me, Isomer B), 147.6, 147.7, 148.3, 148.4 (L: N*C*CH$_2$), 135.9, 136.2, 136.6, 136.9, 137.0, 137.0, 137.3, 137.9, 137.9, 138.1, 138.3, 138.5, 145.1, 145.4, 145.4, 145.6, 146.7, 146.8, 147.0, 147.1, 147.2, 147.9, 148.6, 148.8, 148.9, 149.1, 149.2, 149.5, 149.5, 149.5 (Dipp), 187.4 (IDipp: N*C*N, Isomer A), 187.8 (IDipp: N*C*N, Isomer B).

$^{31}P\{^1H\}$ NMR (161.98 MHz, 300 K, C_6D_6): ABCDEMSX spin system: Isomer A: –237.1 (m, P_A), –190.3 (m, P_B), –162.2 (m, P_C), –149.2 m, P_D), –123.5 (m, P_E), –60.5 (m, P_M), 51.3 (m, P_S), 191.1(m, P_X); Isomer B: –232.2 (m, P_A), –199.3 (m, P_B), –164.8 (m, P_C), –145.0 (m, P_D), –113.7 (m, P_E), –46.5 (m, P_M), 46.4 (m, P_S), 208.8 (m, P_X).

^{29}Si NMR (99.36 MHz, 300 K, C_6D_6): δ / ppm = –3.9 (br), 60.8 (br).

Elemental analysis calcd. for $C_{85}H_{116}N_6Ni_2P_8Si_2$ (Mw = 1643.25 g·mol^{-1}): C 62.13, H 7.12, N 5.11; found C 62.86, H 7.09, N 5.08. The deviation in the carbon content might be explained by small amounts of residual carbene IDipp.

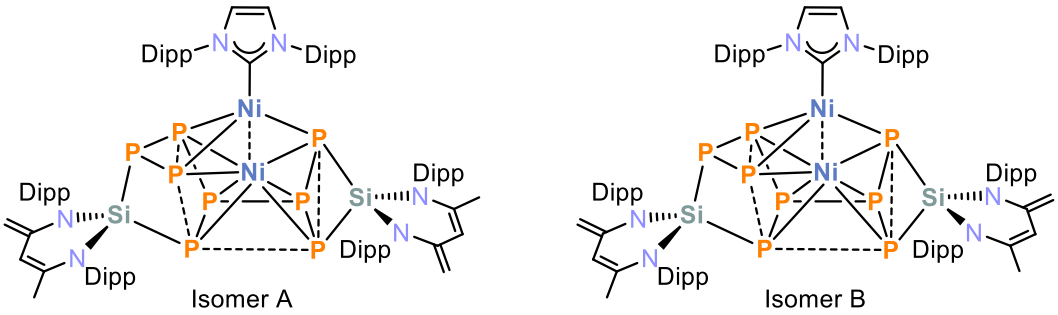

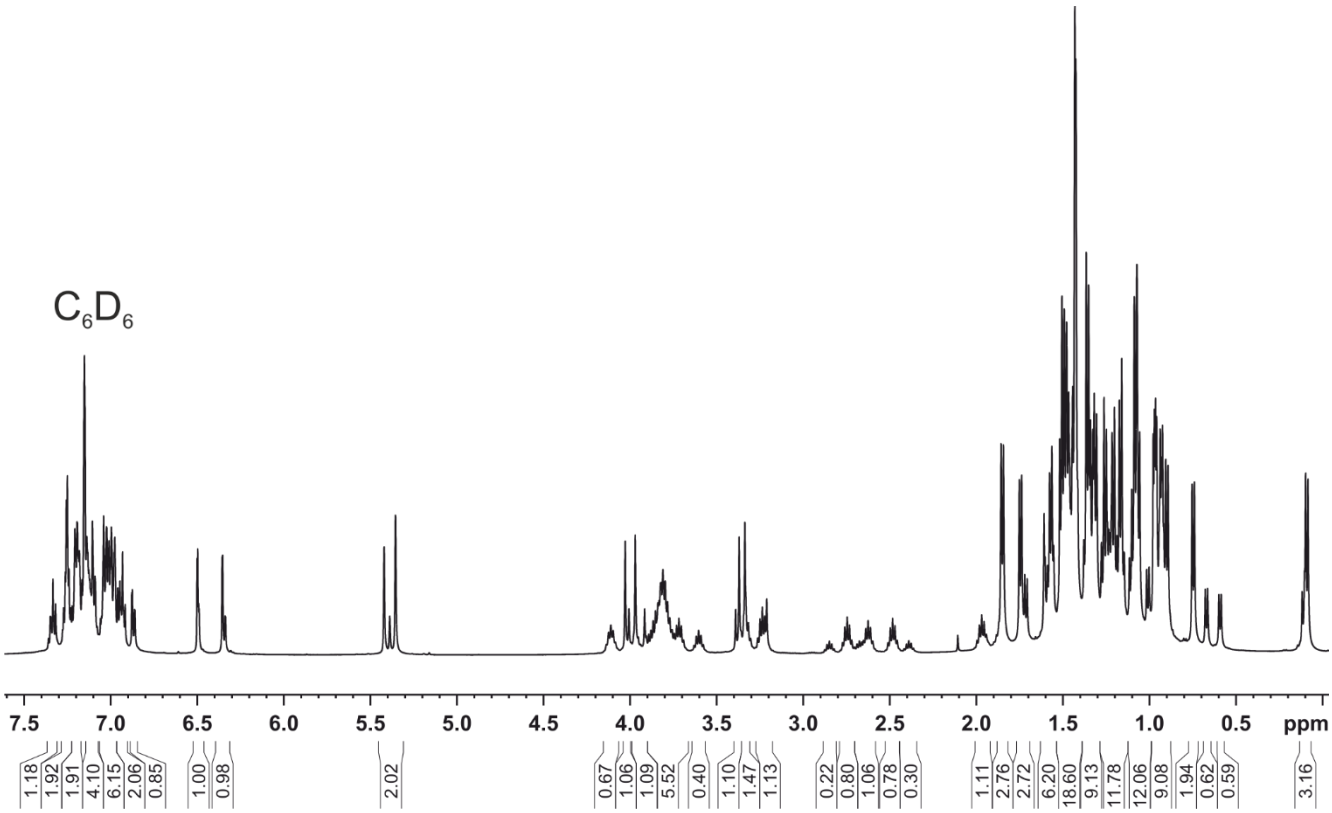

Figure S19. ^1H NMR spectrum (400 MHz, 300 K, C_6D_6) of [(IDipp)$NiP_8\{SiL\}_2$] (**3**).

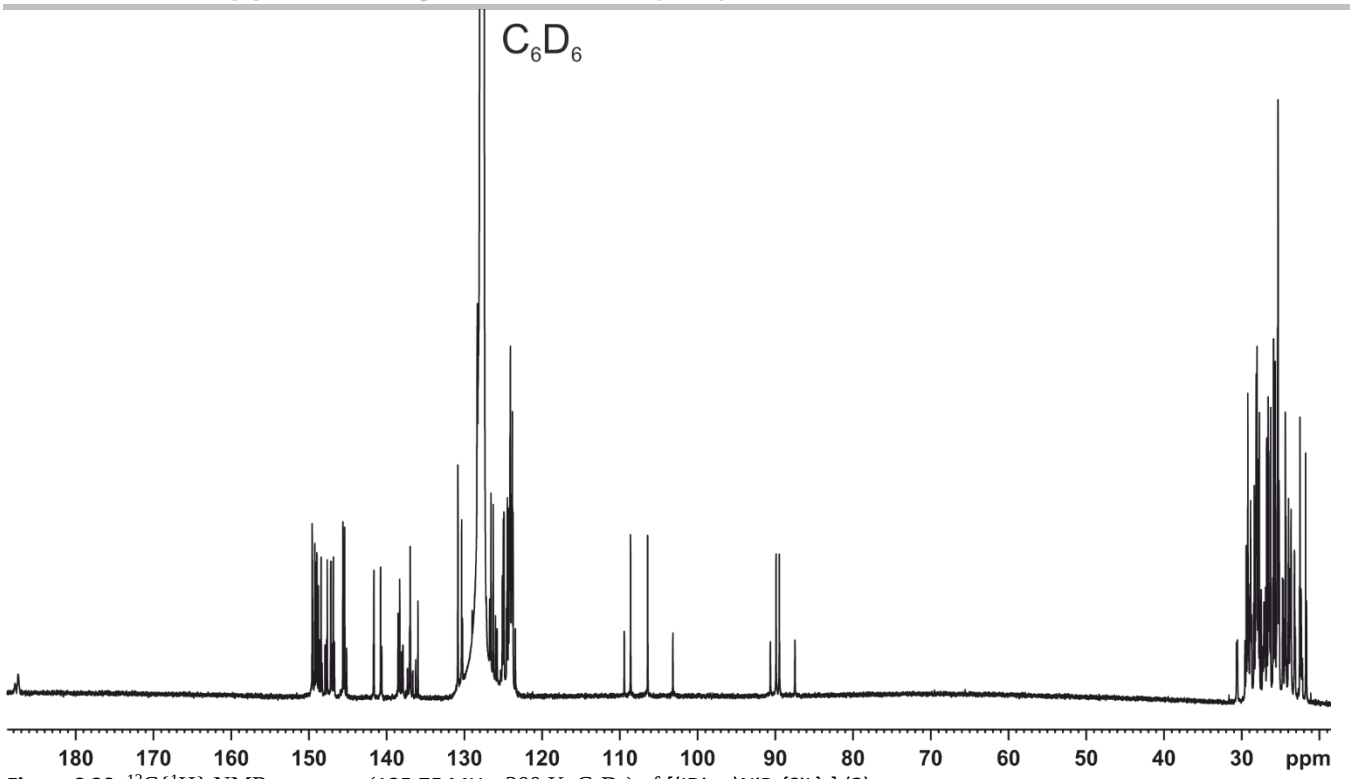

Figure S 20. $^{13}C\{^{1}H\}$ NMR spectrum (125.75 MHz, 300 K, C_6D_6) of [(IDipp)NiP$_8${SiL}$_2$] (**3**).

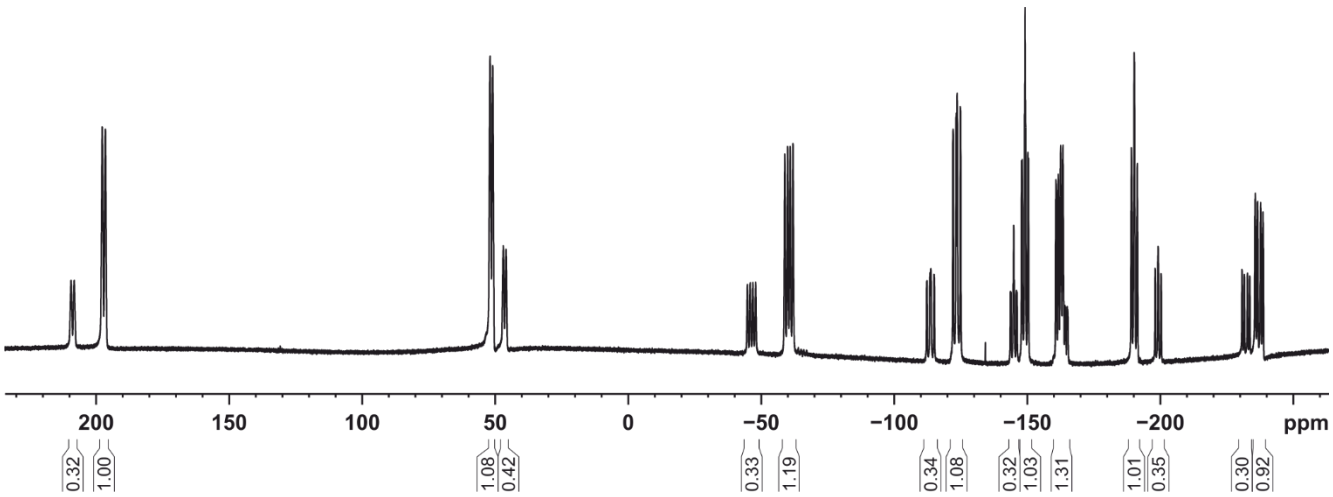

Figure S21. $^{31}P\{^{1}H\}$ NMR spectrum (202.45 MHz, 300 K, C_6D_6) of [(IDipp)NiP$_8${SiL}$_2$] (**3**).

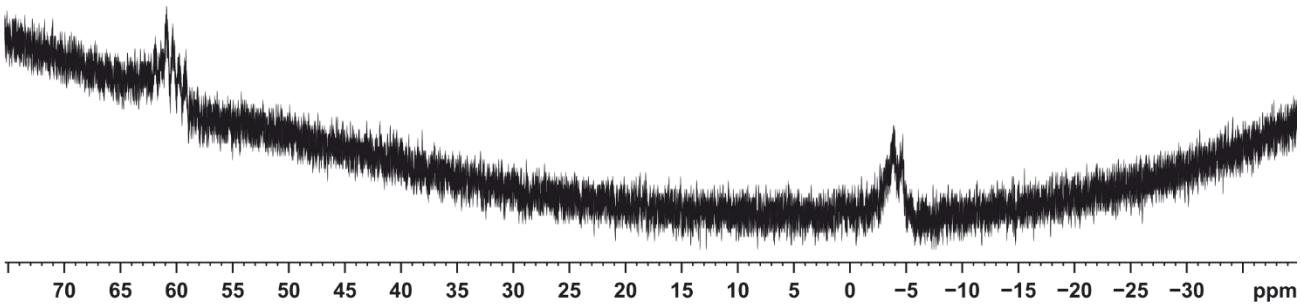

Figure S22. ^{29}Si NMR spectrum (99.36 MHz, 300 K, C_6D_6) of [(IDipp)NiP$_8${SiL}$_2$] (**3**).

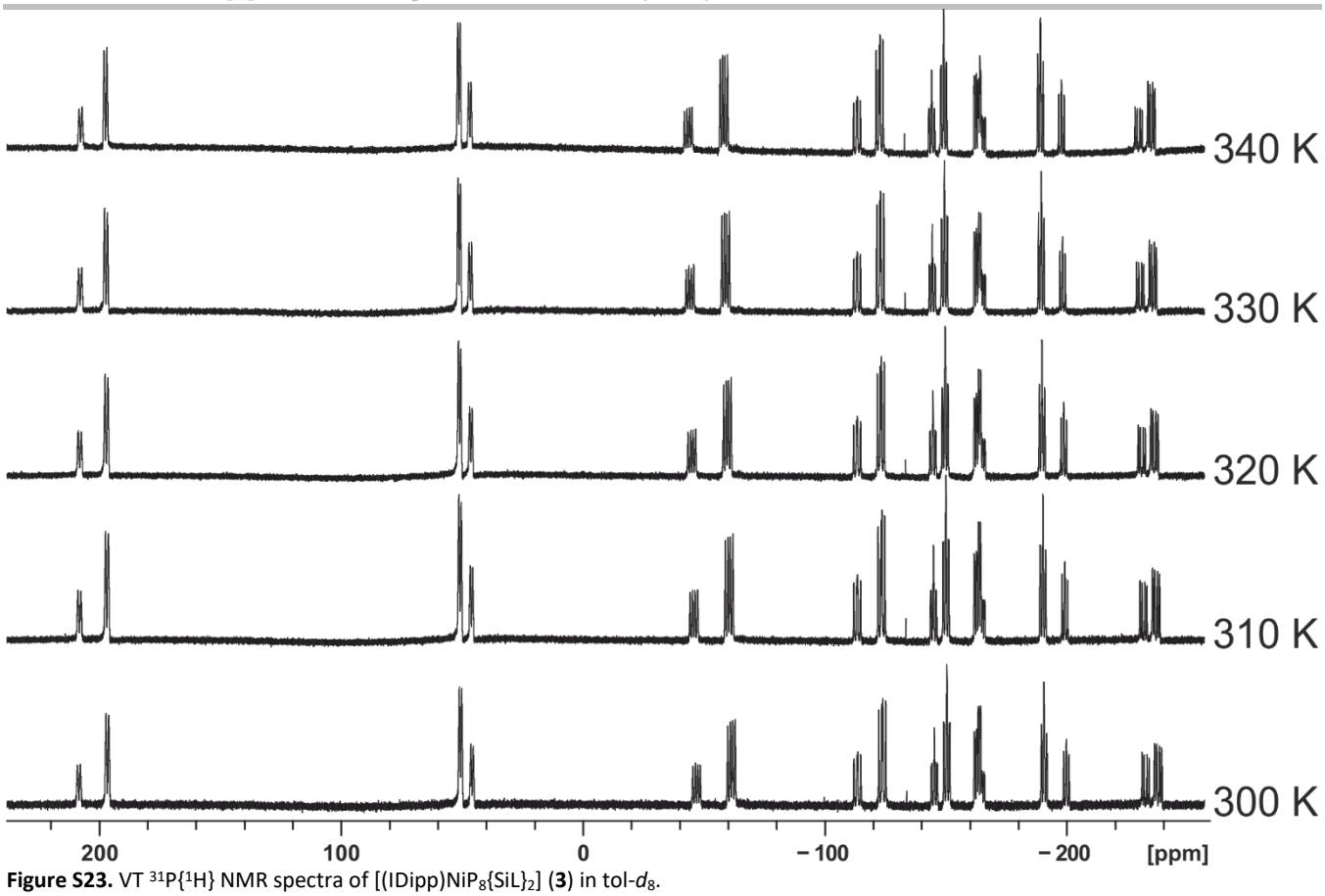

Figure S23. VT $^{31}P\{^{1}H\}$ NMR spectra of [(IDipp)$NiP_8\{SiL\}_2$] (**3**) in tol-d_8.

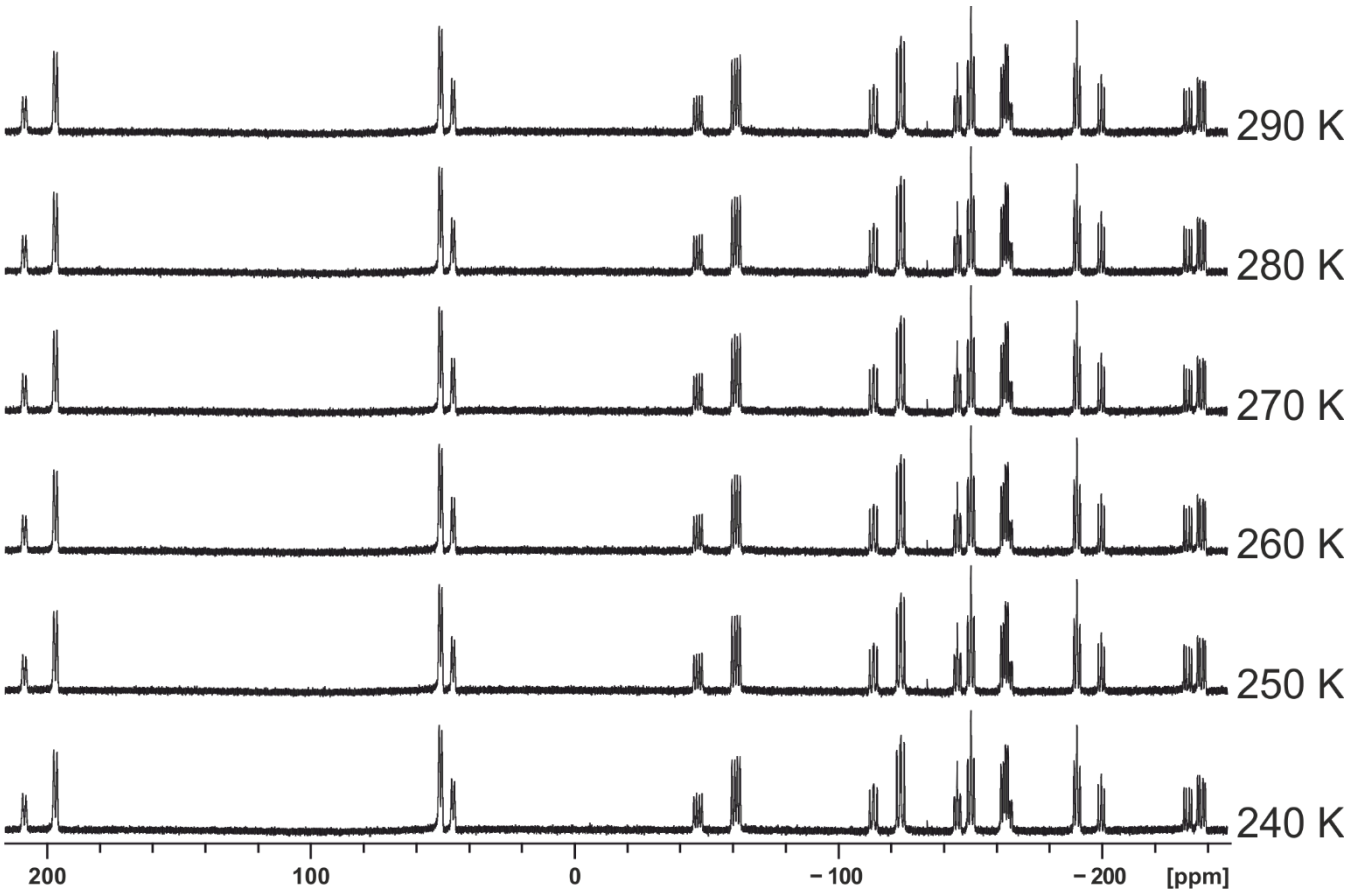

Figure S24. VT $^{31}P\{^{1}H\}$ NMR spectra of [(IDipp)$NiP_8\{SiL\}_2$] (**3**) in tol-d_8.

Table S1. Calculated $J(^{31}P,^{31}P)$ coupling constants (TPSS/pcSseg-2 level of theory) and $J(^{31}P,^{31}P)$ coupling constants obtained by an iterative fitting procedure using the calculated $J(^{31}P,^{31}P)$ coupling constants as starting point. $J(^{31}P,^{31}P)$ coupling constants are given in Hz. Extended signals (upwards) and simulations (downwards) with a representation of the core of the cluster **3**; thermal ellipsoids are drawn at the 40 % probability level (bottom).

Assignment of nuclei	Calculated $J(^{31}P,^{31}P)$	Iterative fitting $J(^{31}P,^{31}P)$	Assignment of nuclei	Calculated $J(^{31}P,^{31}P)$	Iterative fitting $J(^{31}P,^{31}P)$
AB	-9.2	-7.5	BC	-6.2	-14.1
AC	-162.4	-175.8	BD	-248.2	-247.9
AD	-7.1	-13.8	BE	--	--
AE	0.3	28.0	BM	-11.7	-26.8
AM	-388.0	-409.7	BS	-198.9	-204.2
AS	20.8	35.2	BX	33.7	32.2
AX	11.9	17.1	DE	--	--
CD	-7.1	-8.0	DM	201.8	218.1
CE	-294.0	-325.3	DS	43.0	49.3
CM	19.7	19.9	DX	23.0	14.1
CS	26.5	20.9	MS	20.3	35.1
CX	73.1	48.1	MX	39.6	28.0
EM	-40.4	-13.0	SX	61.0	45.2
ES	--	--			
EX	-233.6	-241.6			

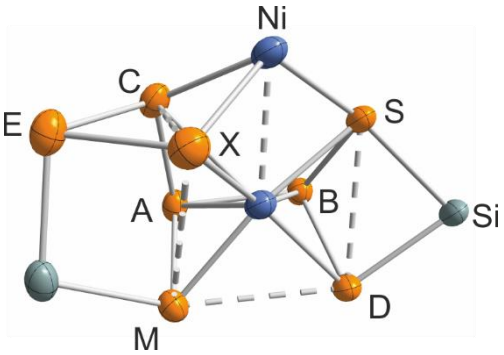

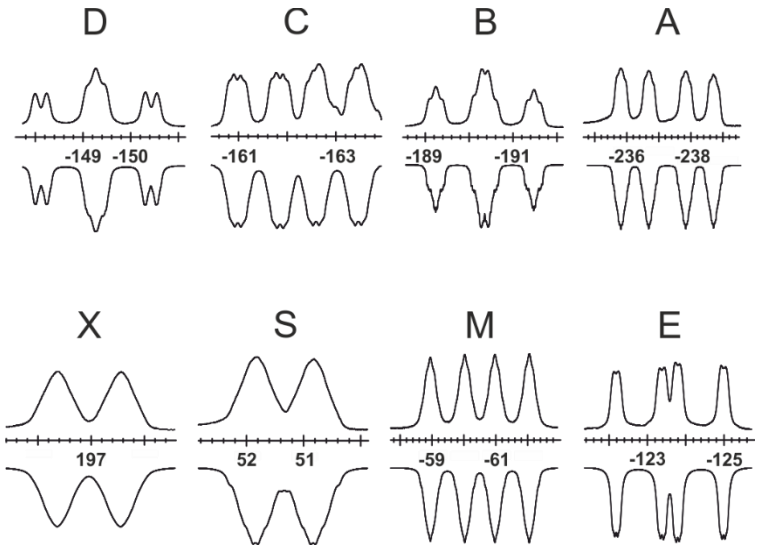

Note on the fitting procedure: The silicon-phosphorus coupling constants were not included in the simulation due to the rather broad signals observed in the experimental $^{31}P\{^{1}H\}$ NMR spectra.

3. Single crystal X-ray diffraction

Crystallographic data were recorded on a Super Nova with a Mikrofocus Cu anode and an Atlas CCD Detector. In all cases, Cu-K_α radiation (λ = 1.54184 Å) was used. Crystals were selected under mineral oil, mounted on micromount loops and quench-cooled using an Oxford Cryosystems open flow N_2 cooling device. The diffraction pattern was indexed and the total number of runs and images was based on the strategy calculation from the program CrysAlisPro (Rigaku, V1.171.40.18b, 2018). The unit cell was refined using CrysAlisPro (Rigaku, V1.171.40.18b, 2018). Either semi-empirical multi-scan absorption corrections[6] or analytical[7] ones were applied to the data. Using Olex2,[8] the structures were solved with SHELXT[9] using intrinsic phasing and refined with SHELXL[10] using least squares refinement on F^2. The hydrogen atoms were located in idealized positions and refined isotropically with a riding model. Crystallographic data for the structures in this paper have been deposited with the Cambridge Crystallographic Data Centre, CCDC, 12 Union Road, Cambridge CB21EZ, UK. Copies of these data can be obtained free of charge (http://www.ccdc.cam.ac.uk) on quoting the depository number: 2009284 (**1a**), 2009285 (**1b**), 2009286 (**2**), 2009287 (**3**).

3.1 Refinement of the solid-state molecular structure of [(IDipp)Ni{(μ-η$^{2:2}$-P$_4$)SiL}$_2$] (1a)

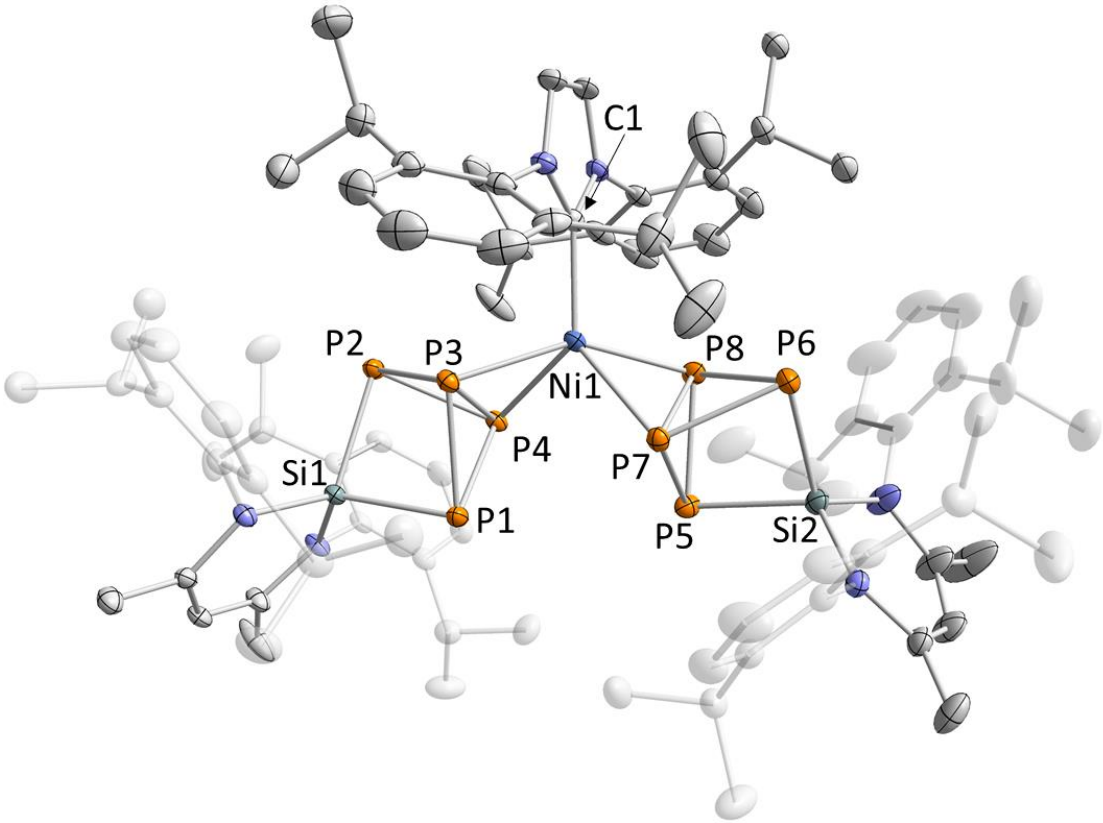

Figure S25. Solid-state molecular structure of **1a**. Hydrogen atoms and solvate molecules are omitted for clarity; thermal ellipsoids are drawn at the 40 % probability level. Selected bond lengths [Å] and angles [°] for **1a**: P1–P3 2.2651 (6), P1–P4 2.2511 (7), P2–P3 2.2565 (7), P2–P4 2.2724 (7), P3–P4 2.2686 (6), Si1–P1 2.2512 (8), Si1–P2 2.2422(7), Ni1–P3 2.2923 (8), Ni1–P4 2.2674 (8), P5–P7 2.2451 (6), P5–P8 2.2603 (7), P6–P7 2.2714 (9), P6–P8 2.2607 (7), P7–P8 2.4749 (7), Si2–P5 2.2475 (9), Si2–P6 2.2455 (6), Ni1–P7 2.2657 (6), Ni1–P8 2.2847 (7), Ni1–C1 1.9761 (16); P1–P3–P2 86.95 (3), P1–P4–P2 86.90 (3), P3–P1–P4 59.54 (2), P3–P2–P4 60.12 (6), P3–Ni1–P4 59.67 (2), P5–P7–P6 86.95 (3), P5–P8–P6 86.85 (2), P7–P5–P8 60.65 (2), P7–P6–P8 60.26 (2), C1–Ni1–P3 105.87 (5), C1–Ni1–P4 131.99 (5), C1–Ni1–P7 128.92 (5), C1–Ni1–P8 104.22 (6).

3.2 Refinement of the solid-state molecular structure of [(IMes)Ni{(μ-η$^{2:2}$-P$_4$)SiL}$_2$] (1b)

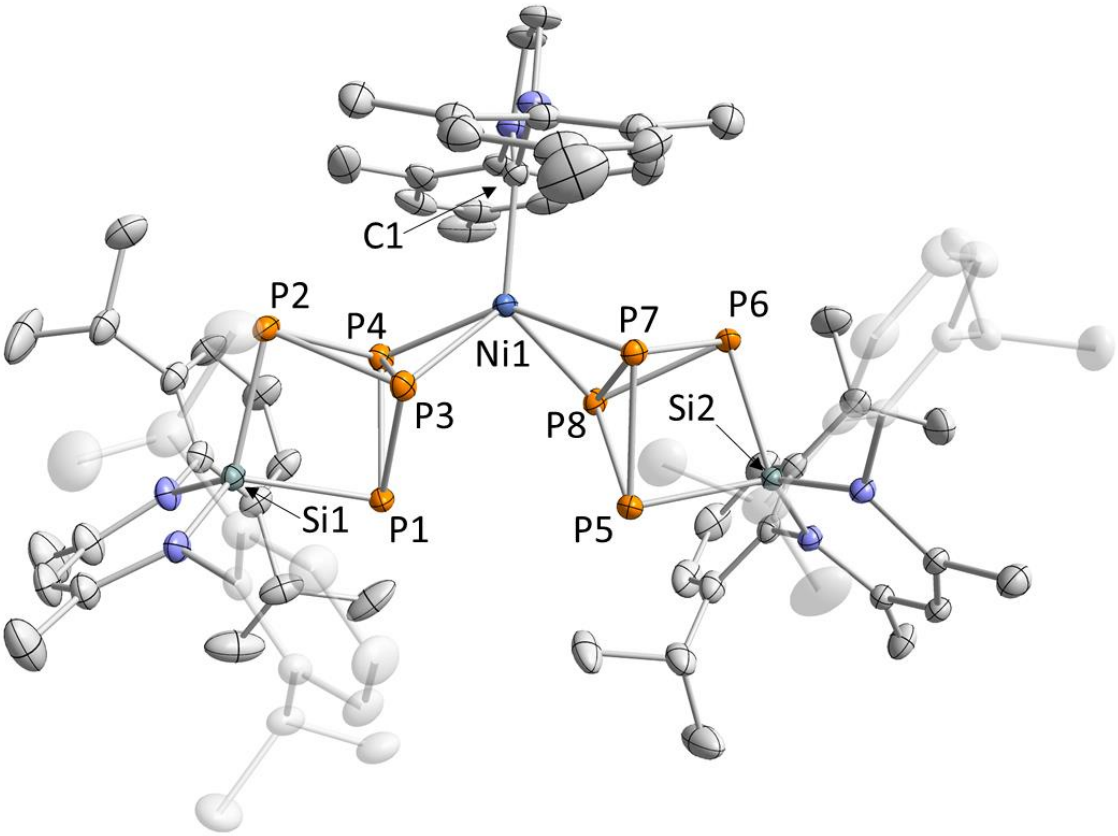

Figure S26. Solid-state molecular structure of **1b**. Hydrogen atoms and solvate molecules are omitted for clarity; thermal ellipsoids are drawn at the 40 % probability level. Selected bond lengths [Å] and angles [°] for **1b**: P1–P3 2.2589 (6), P1–P4 2.2685 (7), P2–P3 2.2652 (7), P2–P4 2.2417 (7), P3–P4 2.2553 (7), Si1–P1 2.2457 (7), Si1–P2 2.2300 (6), Ni1–P3 2.2610 (7), Ni1–P4 2.2531 (7), P5–P7 2.2539 (6), P5–P8 2.2352 (8), P6–P7 2.2594 (8), P6–P8 2.2659 (7), P7–P8 2.2561 (7), Si2–P5 2.2473 (8), Si2–P6 2.2362 (6), Ni1–P7 2.2775 (6), Ni1–P8 2.2482 (6), Ni1–C1 1.957 (2); P1–P3–P2 87.07 (2), P1–P4–P2 87.40 (3), P3–P1–P4 59.76 (2), P3–P2–P4 60.05 (2), P3–Ni1–P4 59.95 (2), P5–P7–P6 86.97 (2), P5–P8–P6 87.26 (3), P7–P5–P8 60.24 (2), P7–P6–P8 59.81 (2), C1–Ni1–P3 124.23 (7), C1–Ni1–P4 105.57 (7), C1–Ni1–P7 112.80 (7), C1–Ni1–P8 126.99 (7).

3.3 Refinement of the solid-state molecular structure of [(IDipp)Ni(μ-η$^{2:2}$-P$_4$)SiL] (2)

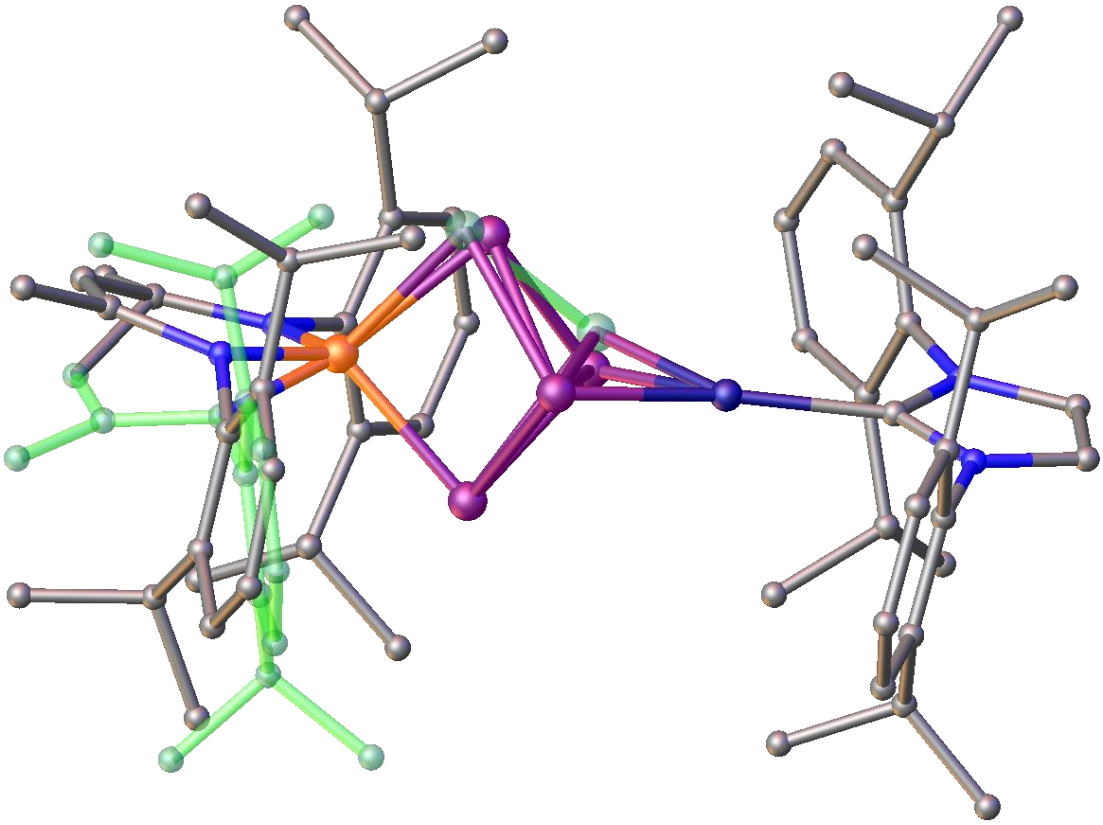

Figure S27. Ball and Stick representation of the solid-state molecular structure of **2**. Hydrogen atoms are omitted for clarity. Disordered part is highlighted in green (PART 2).

The asymmetric unit of the solid-state molecular structure of **2** is disordered over two positions. The occupancy distribution of the backbone of the [LSi] ligand was refined to 82:18 and restrained with a SIMU. Additionally, an AFIX66 was applied the phenylring of the disordered diisopropyphenly group. The bridging P$_4$ unit is also disorder over two positions with crystallographic occupancies of 70:30. The anisotropic displacement factors were restrained with a SIMU.

3.4 Discussion of the structural and NMR spectroscopic data of 2

Complex **2** crystallizes in the orthorhombic space group Pbca. The solid-state molecular structure is presented in Figure S28a and reveals a heterodinuclear [Si(μ-η$^{2:2}$-P$_4$)Ni] core which resembles Driess Ni^{I} complex **D**.[11] Similar to complexes **1a,b** and **D** the conformation of the side-on coordinated [(L)Si(η^2-P$_4$)] moiety remains untouched except for the nickel coordinated P3–P4 bond (2.389 (6) Å) which is about 0.23 Å longer than in the staring material [LSi(η^2-P$_4$)] and even slightly elongated compared to the related compound **D** (2.335 (4) Å).[11] Interestingly, the Ni–P distances (Ni1–P3 2.151 (6), Ni1–P4 2.1223 (10) Å) are considerably shorter than those observed in in complex **D** (Ni1-P3 2.255(4), Ni1-P4 2.277(2) Å).[11] This might be explained by significant back-donation of electron density form the Ni centre toward the phosphorus framework.

The bonding-situation was investigated by means of natural bond orbital analysis (NBO) of the optimized structure of **2**, calculated at the PBE/def2-TZVP level of theory. Looking at the composition of the constructed orbitals five occupied 3d^{10} orbitals together with five two electron two centre P–P bonds were found, suggesting the presence of nickel in its formal oxidation state zero (Figure S31 and S32). By

looking more closely, a strong interaction of a filled Ni(d) orbital with the antibonding σ* orbital of the P3–P4 bond can be observed with a donor-acceptor stabilization energy of 36.5 kcal · mol^{-1} (Figure S28b). This supports the notion that there is strong back-donation of the nickel centre, which is more pronounced in the Ni^0 complex **2** than in the Ni^I compound **D**.[11]

The ^{31}P{^{1}H} NMR spectrum of **2** dissolved in C_6D_6 at room temperature shows three chemically different ^{31}P nuclei resonating at δ(P_A) = –155.1 ppm, δ(P_B) = –138.0 ppm, and δ(P_X) = 147.3 ppm. The two signals shifted to higher field are each split into a doublet of triplets ($^1J(P_A,P_X)$ = –114.2 Hz, $^1J(P_A,P_B)$ = –25.6 Hz) while the low-field shifted signal δ(P_X) shows a pseudo triplet ($^1J(P_X,P_A)$ = –114.2 Hz, $^1J(P_X,P_B)$ = –114.1 Hz), giving rise to an ABX_2 spin system (Figure S17).

Upon coordination of the [(NHC)Ni] fragment the resonances P_A and P_B are shifted to lower field compared to the starting material[4] and to other comparable diamagnetic [LM(η^2-P_4)] (M = Ga,[12] Ge,[13] Zr, Hf[14]) type complexes with a tricyclo[3.1.0]pentane-like structure. The coordination of the nickel atom is also reflected in the $^1J(P_A,P_B)$ coupling constant ($^1J(P_A,P_B)$ = –25.6 Hz) which is about 162.4 Hz smaller in magnitude than in the non-coordinated case ($^1J(P_A,P_B)$ = –188.0 Hz). The recorded ^{29}Si NMR spectrum of **2** in C_6D_6 reveals a broad resonance at δ = –37.1ppm.

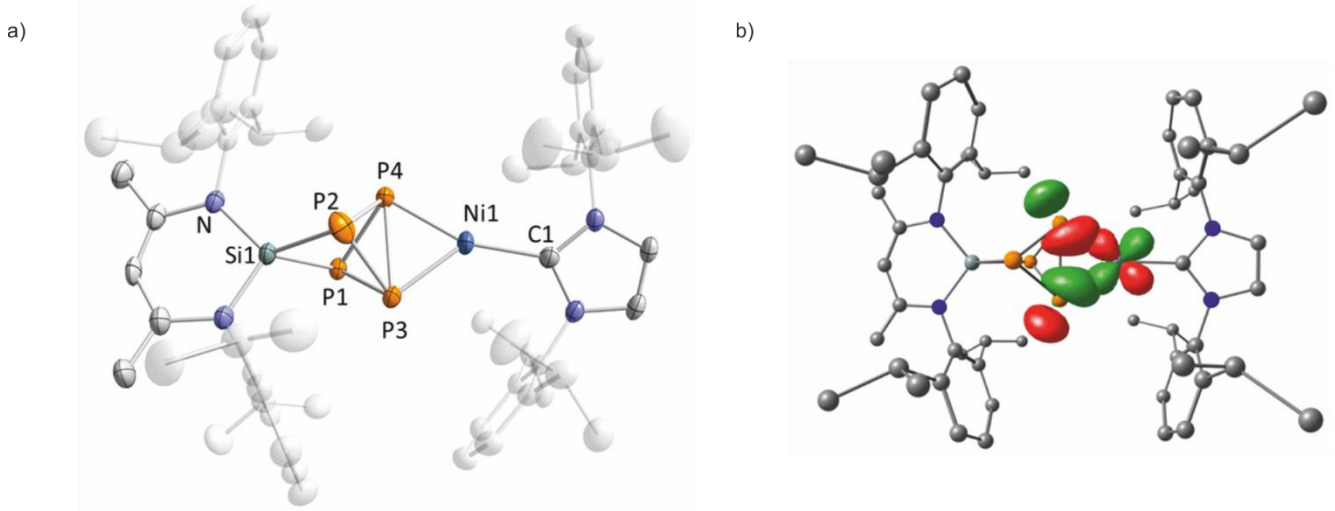

Figure S28. a) Solid-state molecular structure of **2**. Hydrogen atoms and disorder are omitted for clarity; thermal ellipsoids are drawn at the 40 % probability level. Selected bond lengths [Å] and angles [°] for **2** (in case of disorder bond lengths and angles were derived from the part with highest occupancy): P1–P3 2.265 (6), P1–P4 2.244 (6), P2–P3 2.186 (11), P2–P4 2.2469 (14), P3–P4 2.389 (6), Si1–P1 2.249 (5), Si1–P2 2.2235(14), Ni1–P3 2.151 (6), Ni1–P4 2.1223 (10), Ni1–C1 1.930 (3); P1–P3–P2 87.2 (3), P1–P4–P2 86.25 (16), P3–P1–P4 64.0 (2), P3–P2–P4 65.20 (18), P3–Ni1–P4 67.97 (18), C1–Ni1–P3 132.00 (19), C1–Ni1–P4 159.79 (11); b) Natural bond orbitals representing the back-bonding of back-bonding of an occupied Ni d-orbital into the antibonding orbital of the coordinated P−P bond. Ni(d) → σ* (P3–P4) 36.5 kcal · mol^{-1}. Surface isovalue = 0.07. H atoms have been omitted for clarity.

3.5 Refinement of the solid-state molecular structure of [(IDipp)NiP$_8${SiL}$_2$] (3)

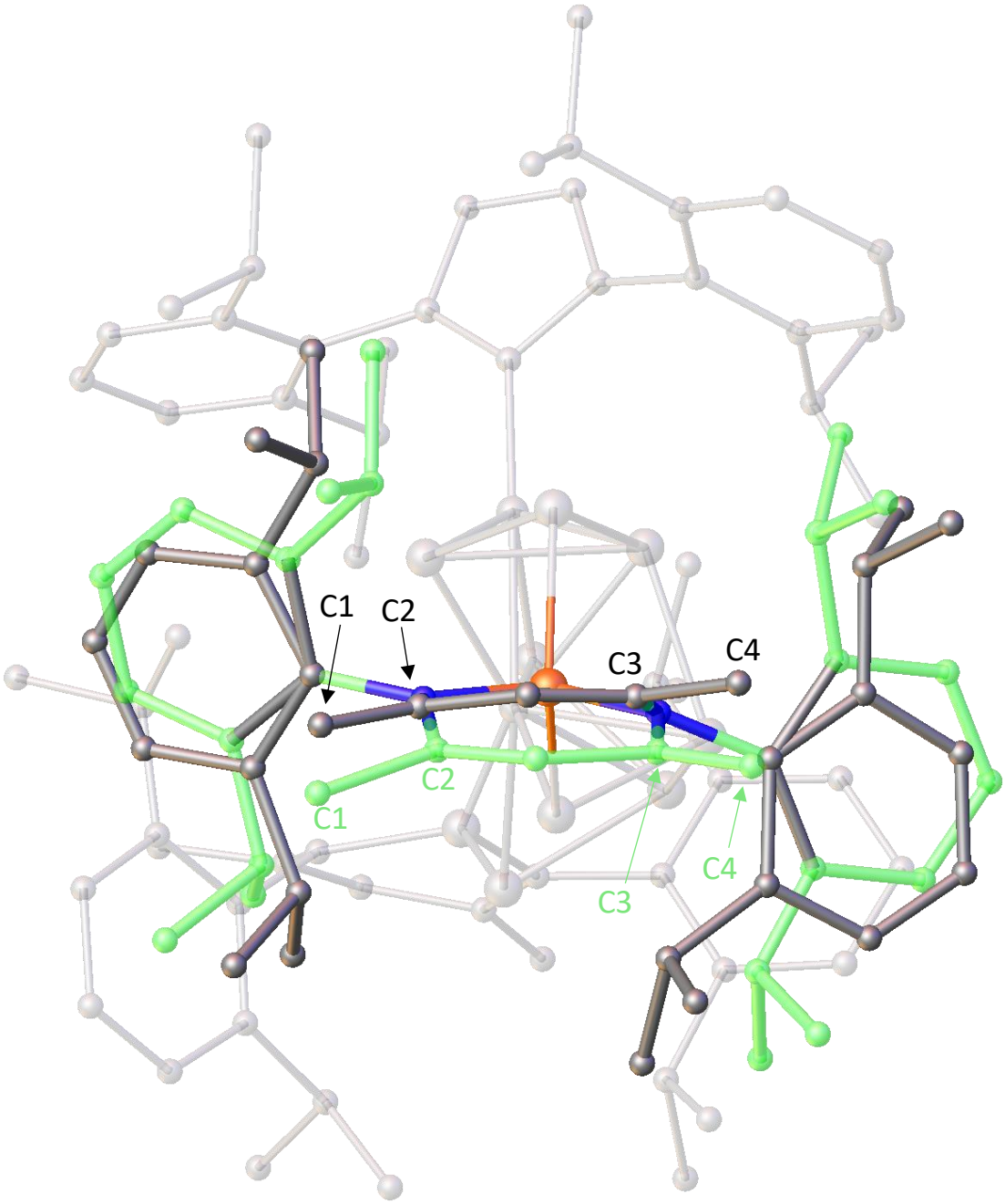

Figure S29. Ball and Stick representation of the solid-state molecular structure of **3**. Hydrogen atoms are omitted for clarity. Disordered part is highlighted in green (PART 2). Selected bond distances [Å] of Part 1: C1–C2 1.350 (9), C3–C4 1.473 (7); Selected bond distances [Å] of Part 2 (highlighted in green): C1–C2 1.57 (3), C3–C4 1.36(2).

The asymmetric unit of the solid-state molecular structure of **3** is disordered over two positions. The occupancy distribution of the backbone of the [LSi] ligand was refined to 73:27 and restrained with a SIMU. Additionally, an AFIX66 was applied the phenylring of the disordered diisopropyphenly group. The disorder of the LSi moiety is likely caused by the presence of two isomers of **3**, which differ in the relative orientation of the C=C double bond in the ligand backbone (Figure S29). A solvent mask was calculated, and 366 electrons were found in a volume of 2140 Å^3 in 2 voids per unit cell. This is consistent with the presence of two *n*-hexane solvent molecules per asymmetric unit, which account for 400 electrons per unit cell.

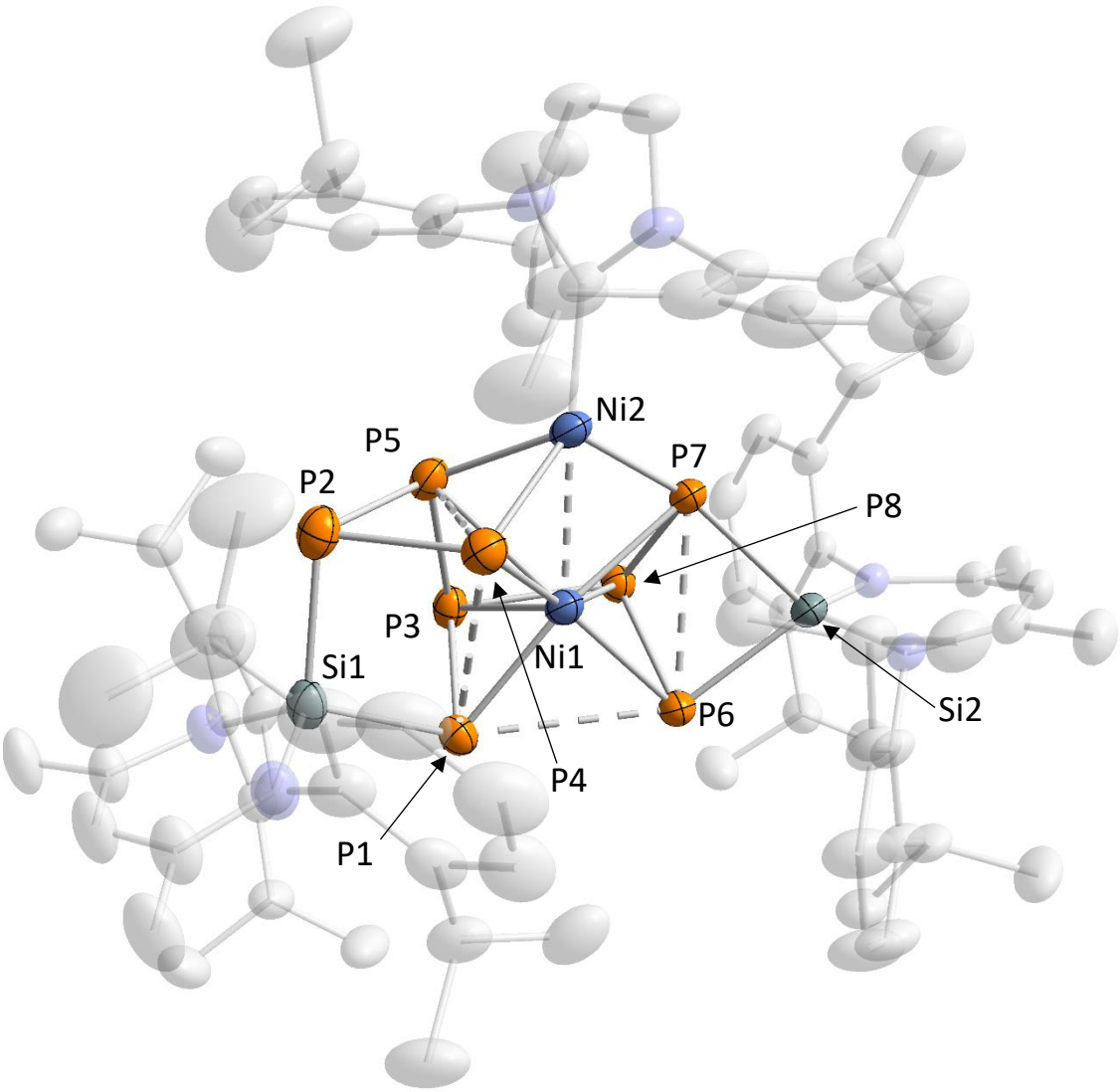

Figure S30. Solid-state molecular structure of **3**. Hydrogen atoms and disorder are omitted for clarity; thermal ellipsoids are drawn at the 40 % probability level. Selected bond distances [Å] and angles [°] for **3**: P1–P3 2.1702 (8), P1···P4 3.4219 (8), P1···P6 3.0176(7), P2–P4 2.2160 (9), P2–P5 2.1704 (10), P4···P5 2.5499 (9), P3–P8 2.4018 (7), P6···P7 2.1946 (7), P7–P8 2.3083 (7), Si1–P1 2.2539 (8), Si1–P2 2.2832 (11), Si2–P6 2.2265 (7), Si2–P7 2.2709 (7), Ni1···Ni2 2.4126 (4), Ni1–P1 2.2717 (6), Ni1–P3 2.4280 (6), Ni1–P6 2.3132 (6), Ni1–P8 2.4143 (6), Ni2–P4 2.1983 (8), Ni2–P5 2.2448 (6), Ni2–P7 2.1811 (7); P1–P3–P8 98.26 (3), P3–P8–P6 97.79 (3), P3–P1–P6 82.91 (2), P3–P1–P4 84.04 (3), P1–P4–P5 68.31 (2), P4–P5–P3 104.92 (4), P2–P4–P5 53.63 (3), P4–P5–P2 55.29 (3), P5–P2–P4 71.08 (3), P5–P3–P8 95.97 (3), P3–P8–P7 107.97 (3), P6–P8–P7 79.88 (3), P8–P7–P6 48.896 (18), P7–P6–P8 51.23 (2), P4–P1–P6 85.977 (19), P1–P6–P7 96.32 (2), P1–Ni1–P4 98.25 (3), P3–Ni1–P5 56.10 (2), P6–Ni1–P7 79.03 (2), P8–Ni–P7 59.00 (2).

Table S2. Crystallographic data for compounds **1a**, **1b**, **2**, and **3**.

Compound	**1a**	**1b**	**2**	**3**
Empirical formula	$C_{91}H_{130}N_6NiP_8Si_2$	$C_{85}H_{118}N_6NiP_8Si_2$	$C_{56}H_{76}N_4NiP_4Si$	$C_{85}H_{116}N_6Ni_2P_8Si_2$
Formula weight	1670.65	1586.50	1015.88	1643.19
Temperature [K]	123.00(10)	123.00(10)	123.00(10)	123.00(10)
Crystal system	monoclinic	monoclinic	orthorhombic	monoclinic
Space group	$P2_1/c$	$P2_1/c$	Pbca	$P2_1/c$
a [Å]	23.6231(4)	17.4813(3)	17.4645(3)	23.3638(5)
b [Å]	13.31130(10)	22.9979(3)	15.4359(3)	16.0951(3)
c [Å]	30.4842(5)	22.0196(3)	42.6490(6)	27.7549(6)
α [°]	90	90	90	90
β [°]	105.741(2)	97.889(2)	90	107.229(2)
γ [°]	90	90	90	90
Volume [$Å^3$]	9226.4(2)	8768.8(2)	11497.3(3)	9968.7(4)
Z	4	4	8	4
ρ_{calc} [g/cm^3]	1.203	1.202	1.174	1.095
μ [mm^{-1}]	2.213	2.303	2.020	2.217
F(000)	3576.0	3384.0	4336.0	3488.0
Crystal size [mm^3]	0.304 × 0.112 × 0.051	0.372 × 0.081 × 0.027	0.32 × 0.107 × 0.088	0.192 × 0.114 × 0.057
Radiation	CuK_α (λ = 1.54184)	Cu K_α (λ = 1.54184)	CuK_α (λ = 1.54184)	Cu K_α (λ = 1.54184)
2Θ range for data collection [°]	7.292 to 148.682	7.182 to 146.22	6.542 to 147.986	6.668 to 148.204
Index ranges	-29 ≤ h ≤ 28, -16 ≤ k ≤ 10, -37 ≤ l ≤ 37	-21 ≤ h ≤ 16, -28 ≤ k ≤ 26, -24 ≤ l ≤ 27	-21 ≤ h ≤ 20, -18 ≤ k ≤ 16, -52 ≤ l ≤ 52	-28 ≤ h ≤ 28, -19 ≤ k ≤ 14, -34 ≤ l ≤ 34
Reflections collected	55783	41046	46160	58661
Independent reflections	18506 [R_{int} = 0.0253, R_{sigma} = 0.0258]	16774 [R_{int} = 0.0293, R_{sigma} = 0.0362]	11392 [R_{int} = 0.0388, R_{sigma} = 0.0307]	19509 [R_{int} = 0.0257, R_{sigma} = 0.0254]
Data / restraints / parameters	18506/6/1033	16774/146/984	11392/468/769	19509/654/1183
Goodness-of-fit on F^2	1.015	1.018	1.137	1.029
Final R indexes [I>=2σ (I)]	R_1 = 0.0334, wR_2 = 0.0816	R_1 = 0.0390, wR_2 = 0.0939	R_1 = 0.0664, wR_2 = 0.1626	R_1 = 0.0446, wR_2 = 0.1149
Final R indexes [all data]	R_1 = 0.0397, wR_2 = 0.0854	R_1 = 0.0518, wR_2 = 0.1021	R_1 = 0.0759, wR_2 = 0.1680	R_1 = 0.0533, wR_2 = 0.1215
Largest diff. peak/hole [e $Å^{-3}$]	0.50/-0.51	0.53/-0.59	0.70/-0.62	0.78/-0.35

4. Theoretical investigations

4.1 Computational Methods

All calculations were performed with the ORCA program package[15] and were conducted in the gas phase. The RI[16] approximation was used for GGA calculations whereas the RIJCOSX[17] approximation was used for hybrid-DFT calculations. Geometry optimisations have been carried out at the PBE/def2-TZVP[18,19,20] level of theory and the nature of stationary point was confirmed by a numerical frequency analysis. For compound **3**, a model **3'** in which the *iso*-propyl substituents of at the diisopropylphenyl moieties have been truncated to methyl groups. The higher occupied part of the single X-ray crystals structure was chosen as initial geometry for **3'**.

4.2 NBO Analysis of complex 2

An NBO(version 6.0)[21] analysis was carried out using the Gaussian 09 program package[22] (using the ORCA PBE singlet geometry, and using the def2-TZVP basis). The donor properties of the nickel atom in complex **2** were quantified in a second order perturbation theory analysis.

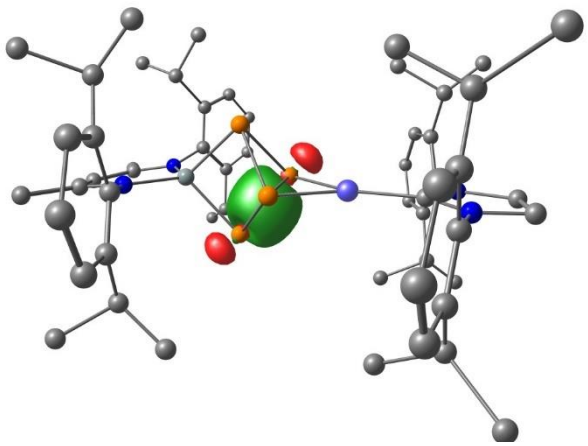

112

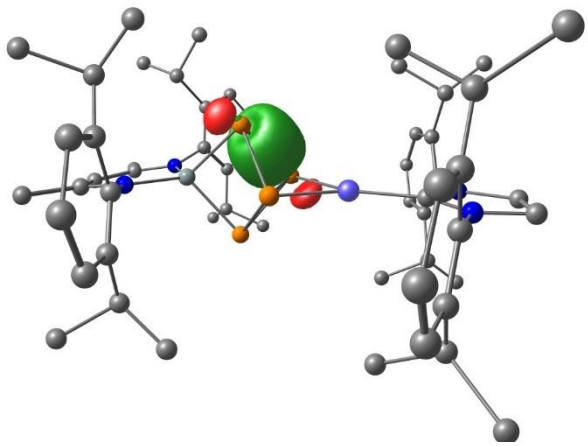

113

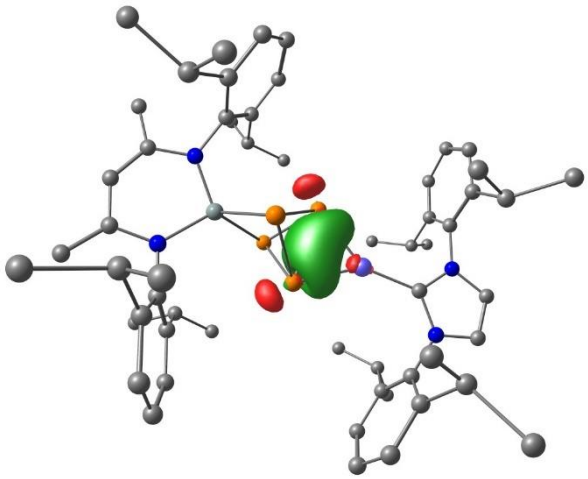

114

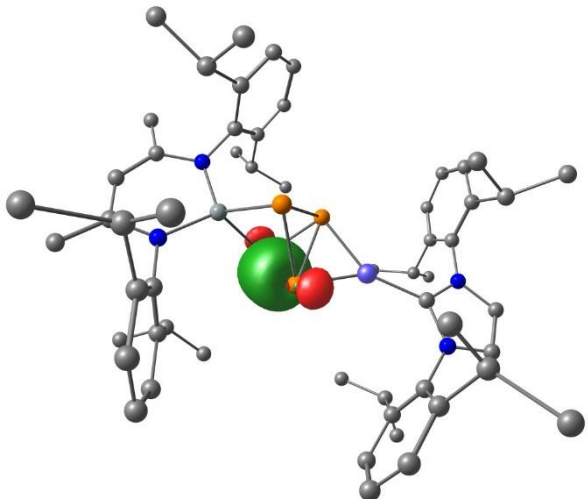

115

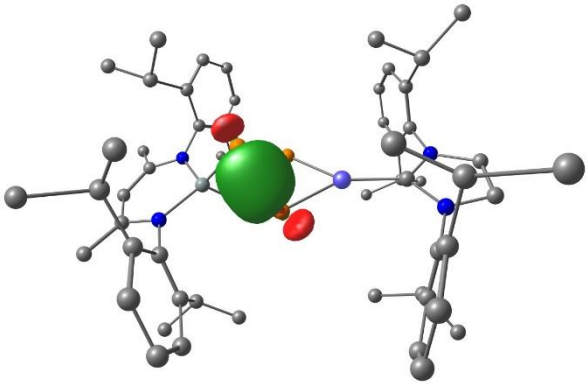

116

Figure S 31. Natural bond orbitals of **2** showing five P–P bonds. Surface isovalue = 0.07. H atoms have been omitted for clarity.

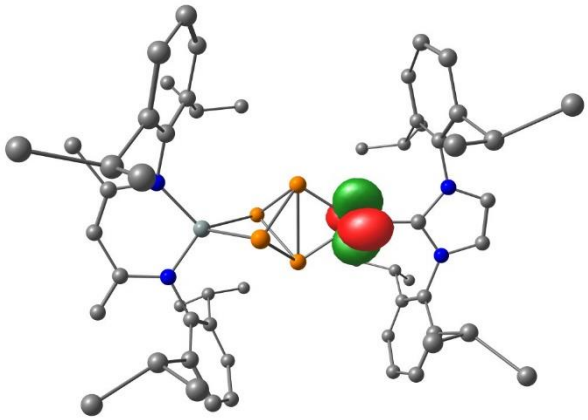

95

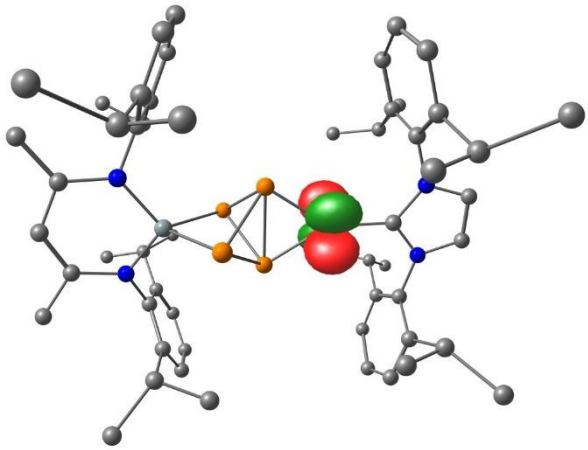

96

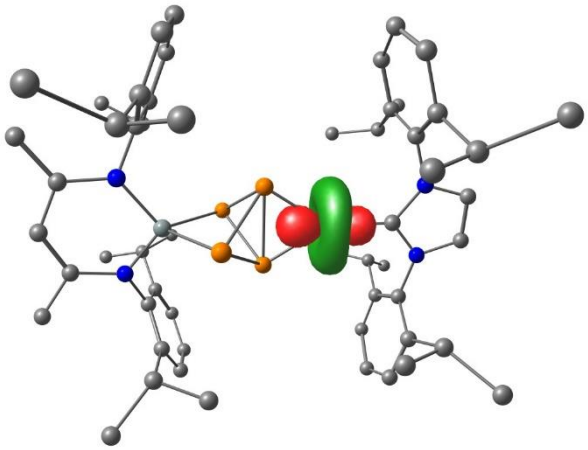

97

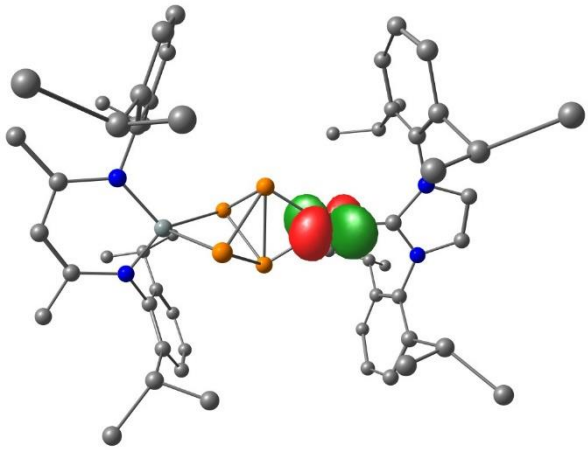

98

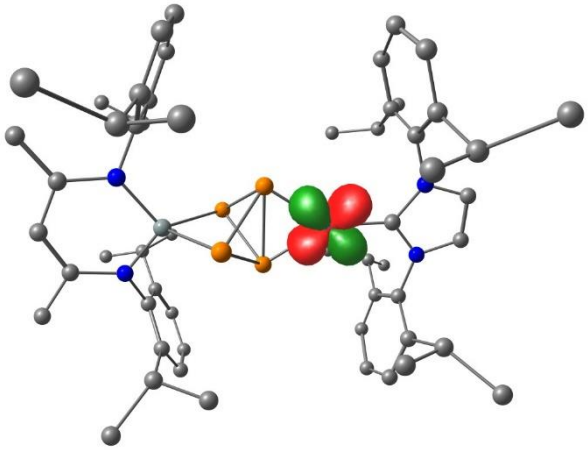

99

Figure S32. Natural bond orbitals of **2** showing five occupied Ni 3d-orbitals. Surface isovalue = 0.05. H atoms have been omitted for clarity.

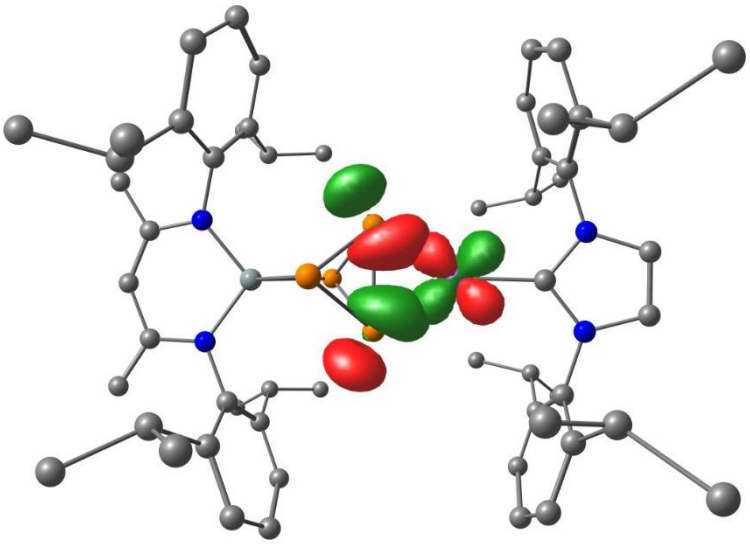

Figure S33. Natural bond orbitals representing the back-bonding of back-bonding of an occupied Ni d-orbital into the antibonding orbital of the coordinated P−P bond. Ni(d) → σ* (P1–P2) 36.5 kcal · mol^{-1}. Surface isovalue = 0.07. H atoms have been omitted for clarity.

4.3 Intrinsic bond orbital analysis of compound 3′

Intrinsic bond orbitals (IBO) have been constructed from the occupied PBE orbitals according to Knizia *et al*.[23] To investigate the bonding interactions within the cluster we analysed the composition and shape of the respective IBOs. Thereby, IBOs with a Ni contribution greater than 70% were assigned to be occupied 3d orbitals. This criterion ensures that only significant bonding interactions between the cluster atoms are considered. Orbitals with comparatively low Ni contribution 71% to 73% may be explained by a significant back-donation of electron density from the Ni atoms to the electron-deficient cluster.

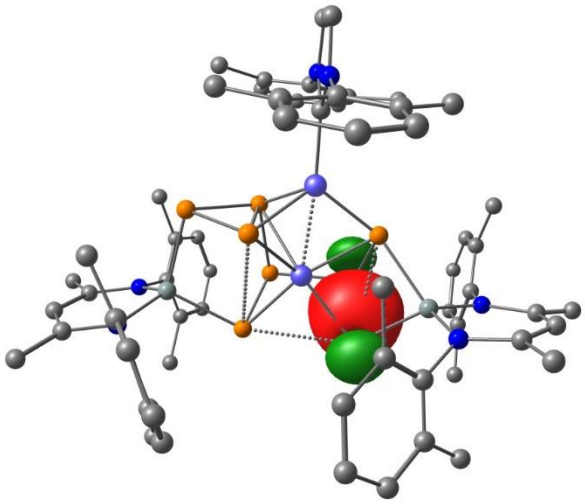

150

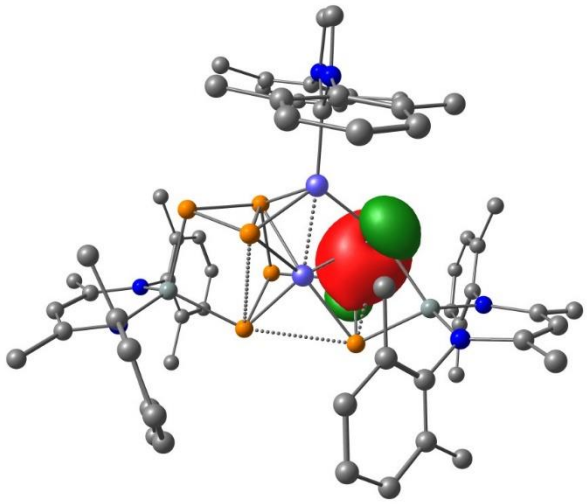

152

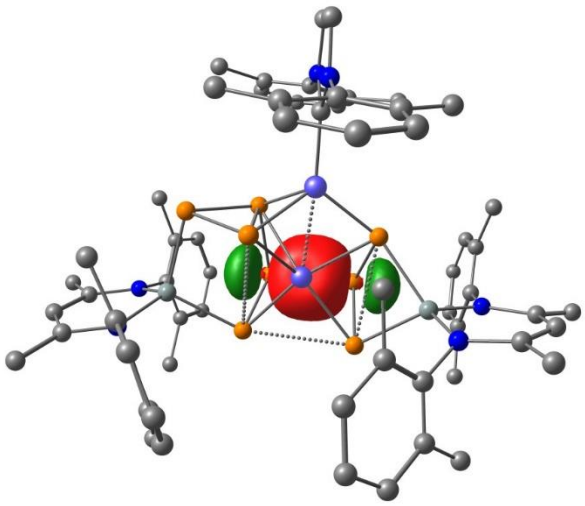

153

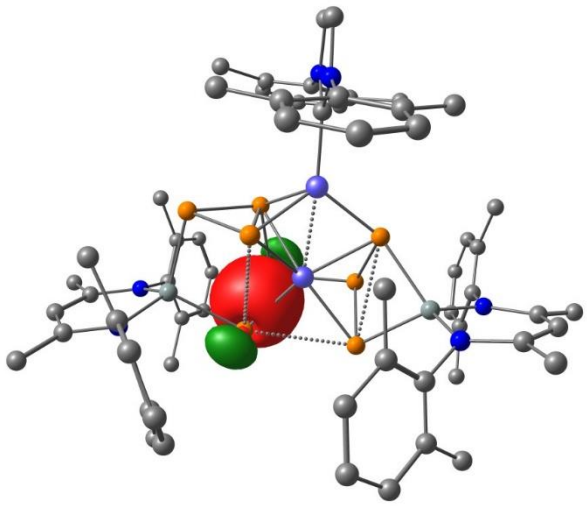

154

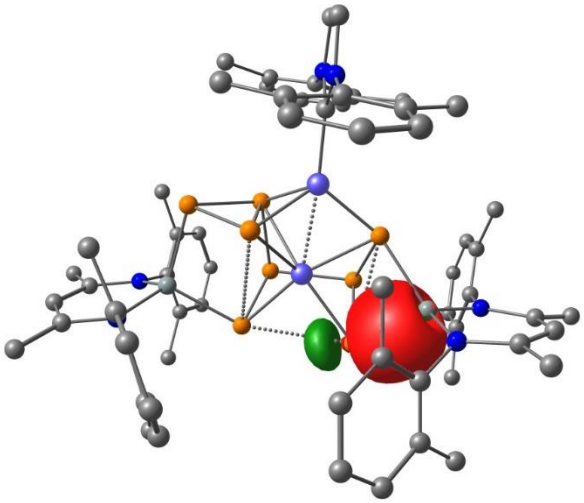

156

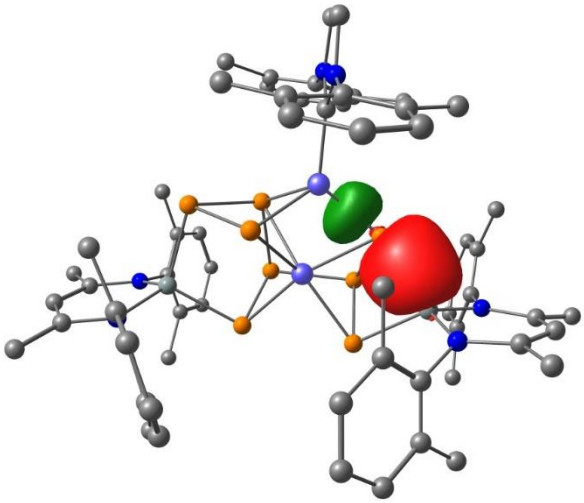

157

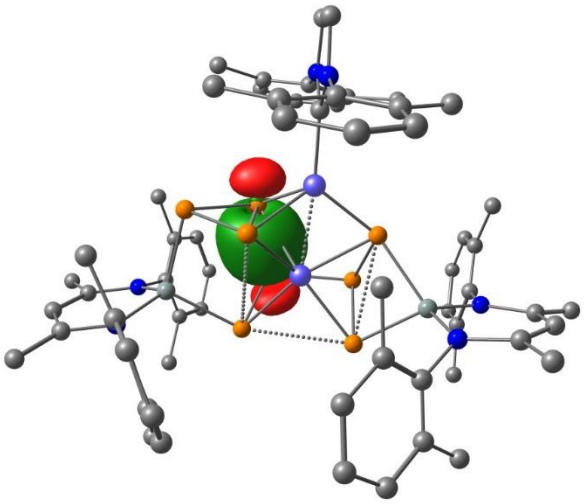

158

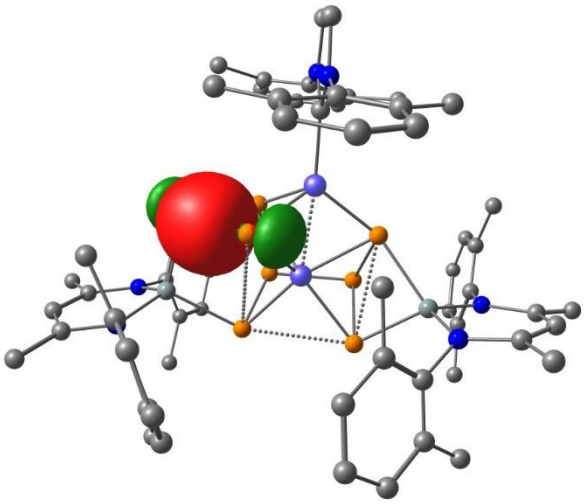

159

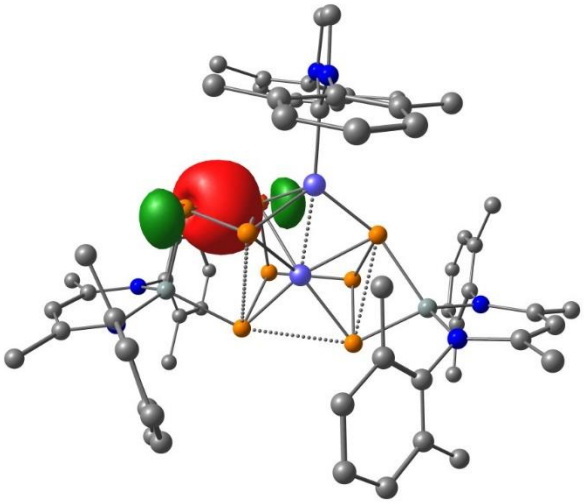

160

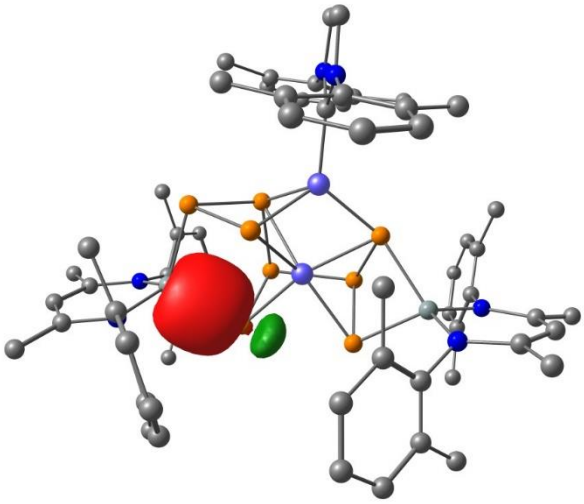

161

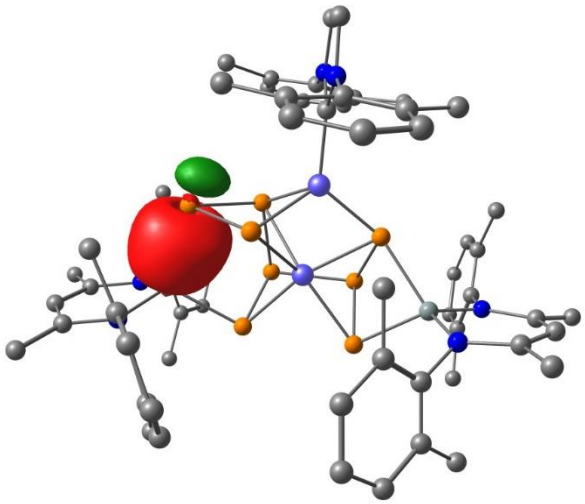

162

Figure S34. Intrinsic bond orbitals of **3'** showing 2-centre-2-electron bonding interactions between the cluster atoms. Surface isovalue = 0.05. H atoms have been omitted for clarity.

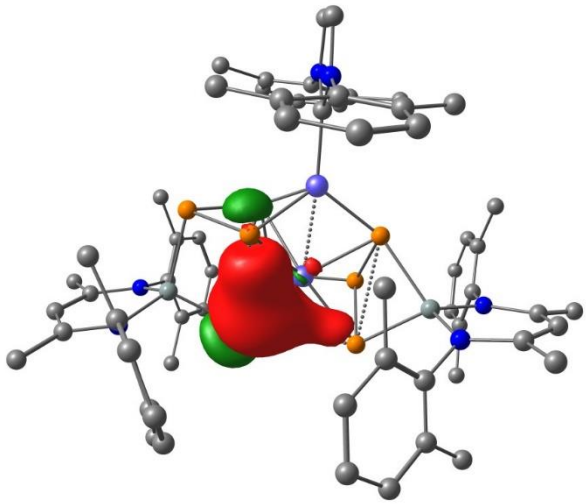

320

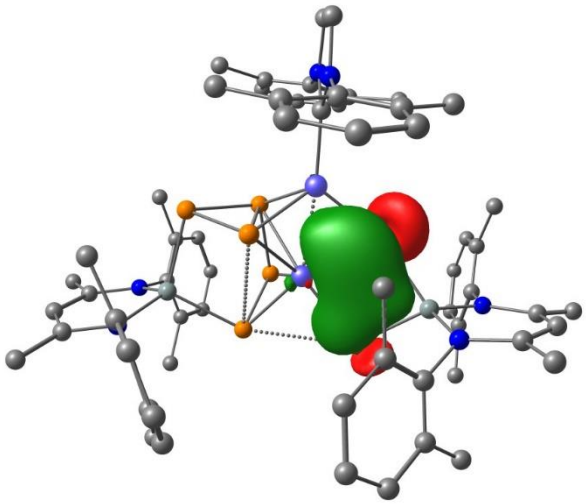

337

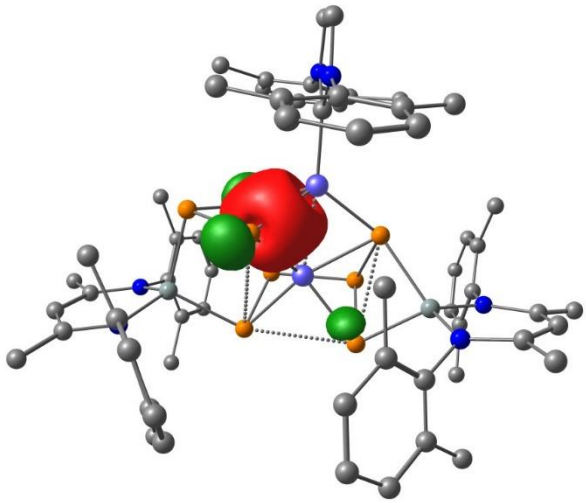

339

Figure S35. Intrinsic bond orbitals of **3'** multicentre bonding interactions between the cluster atoms. Surface isovalue = 0.05. H atoms have been omitted for clarity.

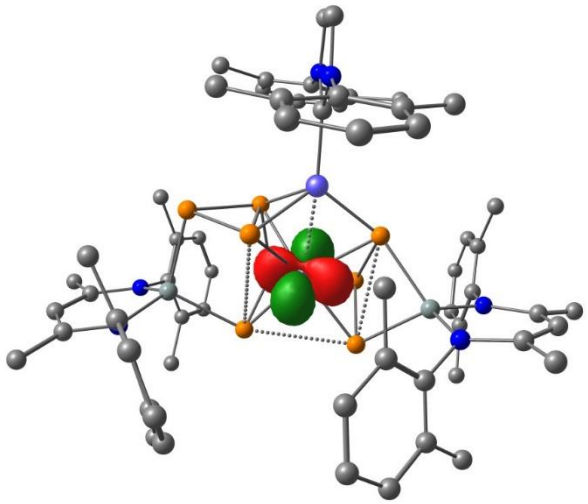

9 (96% Ni)

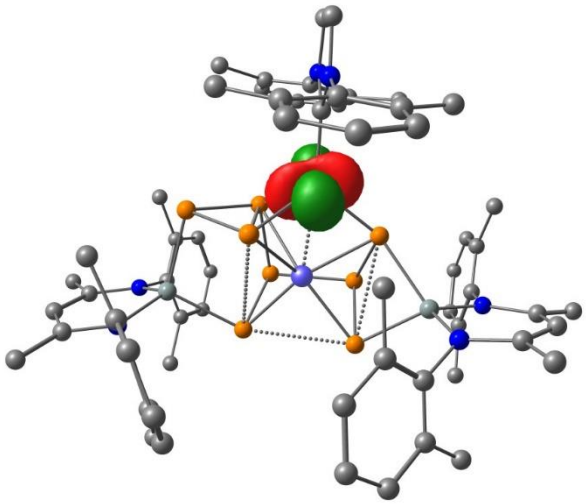

19 (96% Ni)

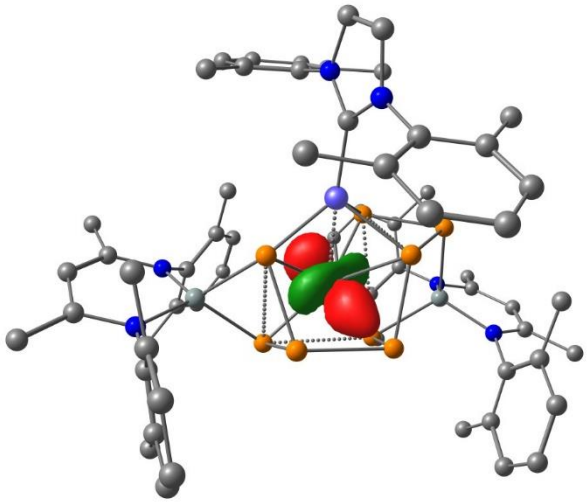

144 (93% Ni)

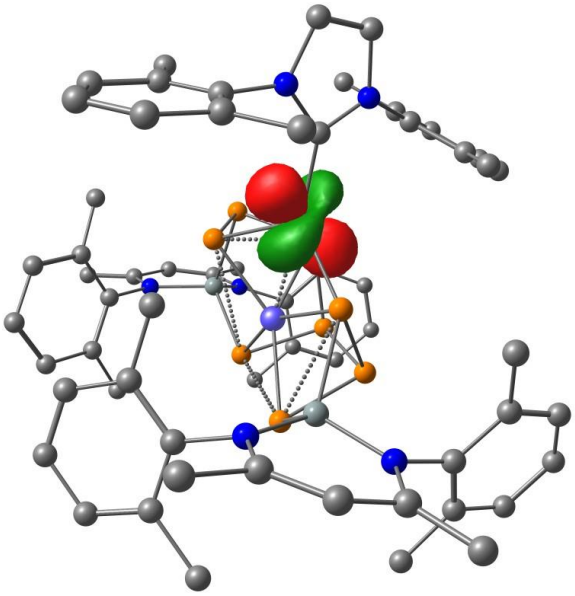

145 (94% Ni)

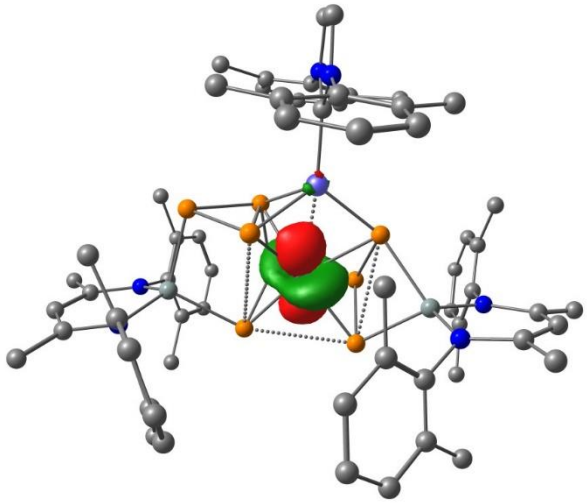

146 (91% Ni)

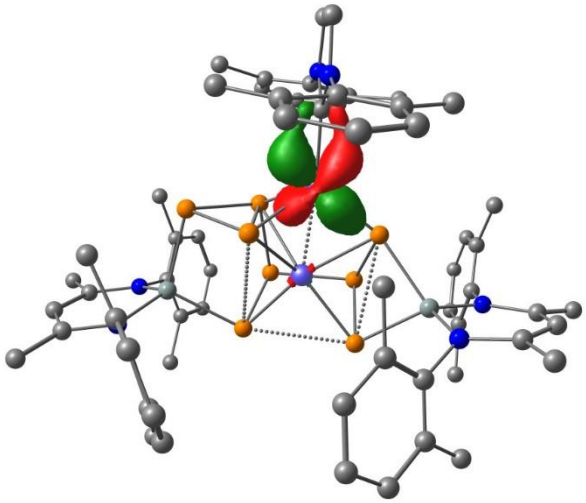

147 (89% Ni)

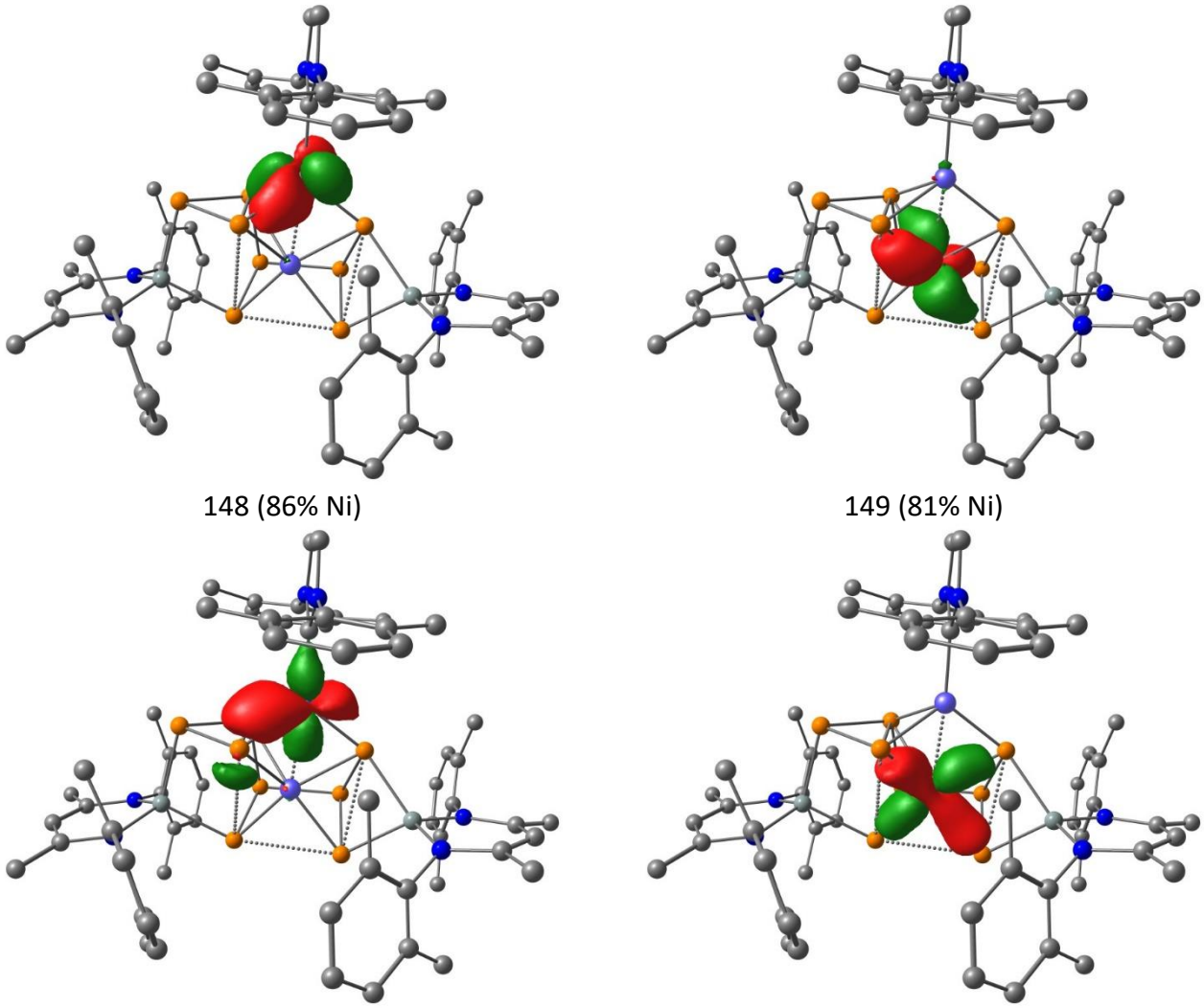

148 (86% Ni) 149 (81% Ni)

155 (71% Ni) 319 (73% Ni)

Figure S36. Intrinsic bond orbitals of **3'** showing the filled 3d-orbitals at the Ni atoms (highest contribution of a single Ni atom is given in parentheses). Surface isovalue = 0.05. H atoms have been omitted for clarity.

Calculation of ^{31}P NMR shieldings

The chemical shielding constants of the optimized geometries of complexes **2** and **3'** and were calculated at the TPSS/pcSseg-2 level of theory.[24,25] Calculated coupling constants are given in Table S1, *vide supra*.

Table S3. Calculated chemical shielding constants and chemical shifts of **3'**. Complex **2** was used as reference. Representation and assignment of ^{31}P nuclei of core of **3** (bottom).

assignment of the ^{31}P	isotropic shielding constant	calculated chemical shift [ppm]	experimental chemical shift [ppm]	absolute deviation from the experimental values
A	545.167	-233.5	-236.7	3.2
B	504.562	-192.9	-189.8	3.1
C	444.44	-132.7	-161.4	28.7
D	439.386	-127.7	-148.5	20.8
E	396.255	-84.5	-122.8	38.3
M	361.048	-49.3	-59.7	10.4
S	244.308	67.4	51.9	15.5
X	87.693	224.0	197.7	26.3

Table S4. Calculated chemical shielding constants and chemical shifts of **3'**. Complex **2** was used as reference. Representation and assignment of ^{29}Si nuclei of core of **3** (bottom).

assignment of the ^{29}Si	isotropic shielding constant	calculated chemical shift [ppm]	experimental chemical shift [ppm]	absolute deviation from the experimental values
Si1	360.958	-8.6	-3.9	4.7
Si2	294.852	57.5	60.8	3.3

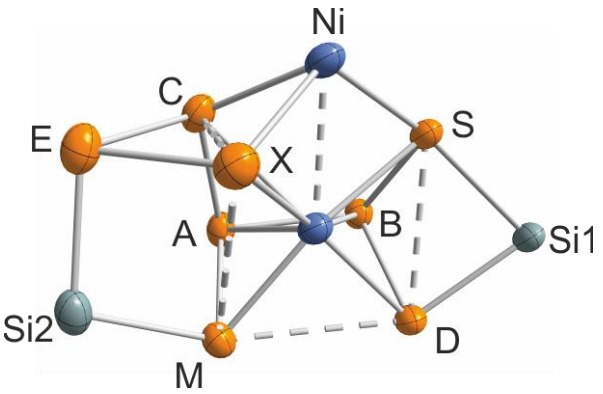

Table S5. Calculated chemical shielding constants and chemical shifts of reference system **2**. Representation and assignment of ^{31}P nuclei of core of **2** (bottom).

assignment of the ^{31}P and ^{29}Si nuclei	isotropic shieling constant	calculated chemical shift [ppm]	experimental chemical shift [ppm]	absolute deviation from the experimental values
P1	148.7	163.0	147.3	15.7
P2	164.4	reference	147.3	0.0
P3	468.6	-156.9	-138.0	18.9
P4	489.2	-177.5	-155.1	22.4

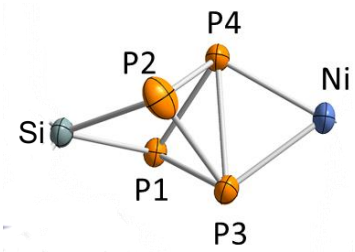

Cartesian Coordinates of Optimized Structures

Cartesian coordinates of the optimized gas phase geometry of the complex **2** (PBE/def2-TZVP, S= 0)

Ni	7.04674659858483	7.77380192561013	25.95004525916821
Si	9.42411136763949	11.42440432603290	27.44306874250845
P	8.29946996869168	9.45075309790504	25.41415003450989
P	7.30926338697802	11.04394117932097	26.71892808243584
P	9.87052737160240	9.23777923580356	27.04900529004216
P	7.67347323011013	8.97533710856267	27.62965200103657
N	5.84922695366098	5.75176064802026	24.11778150849454
N	5.36411844088936	5.33073450702456	26.17438532961149
N	9.60749592260333	11.96471264953618	29.11203950327963
C	6.38289110092842	6.36728542874326	22.92736274254545
C	6.04850881715092	6.23071115646047	25.39145269493477
N	10.36787462879715	12.61455122053654	26.52261729076772
C	9.11287071446023	11.11817375469191	30.17672998871487
C	4.76625181760074	4.33514696075697	25.41435950134098
H	4.18416293411810	3.53786615127133	25.86121274172554
C	4.20939508725900	6.12937023187050	28.18579955735599
C	5.07278745140863	4.60108286833123	24.11440234801167
H	4.81196562060927	4.08237736441493	23.19948512523417
C	5.27784417229504	5.41097488690136	27.61226967408099
C	7.78790913578659	11.28553847182430	30.65544427914755
C	9.98458258368918	10.16791337470641	30.76867640046171
C	7.65046091938277	5.95902220779767	22.46566746386945
C	5.61132015229006	7.34547993387679	22.26815157107801
C	6.26224895774307	4.76345643040253	28.38560170007807
C	4.15142874990748	6.19192304705052	29.58395702351892
H	3.34253377309090	6.74874085400559	30.06063889217476
C	10.84116367450554	12.27231560087542	25.19626341104923
C	10.09372905174045	12.62770729566998	24.04382244090683
C	6.83132649541612	12.33791699109498	30.10740513094145
H	7.26485303460718	12.72912994040556	29.17448613389487
C	3.15983877987073	6.84676642668255	27.34974134185663
H	3.34132753958628	6.59927628205284	26.29327123552740
C	10.60357282003821	12.27416298010641	22.78614217149041
H	10.03737256908611	12.53961767489080	21.89096807548109
C	4.25512333531782	7.80486543600117	22.78245693247280
H	3.98523501295557	7.16978609903067	23.63922151538369
C	6.15164871736355	7.92115107552500	21.11100343863953
H	5.58377774226253	8.68811145700852	20.58097507535985
C	7.40181288869809	7.53858137613724	20.63152612383822
H	7.80513510366215	8.00322194859336	19.72985489407803
C	7.35427520910689	10.46897790717632	31.70896410484486
H	6.33648352960505	10.58411117278380	32.08649868349347
C	11.44147366014708	10.00836686514950	30.35051891765110
H	11.57486694887234	10.54875538411912	29.40108215544419
C	7.42474582810610	4.00192317279300	27.76616190822924
H	7.28470088262652	3.99897952900270	26.67503069088615
C	6.15392255801080	4.85956778254312	29.77889782878109
H	6.90545677408554	4.37818470886738	30.40744517776874
C	8.49294251418387	4.91993363637269	23.19040341889643
H	7.90264968392212	4.53480550997056	24.03495215852408
C	5.11220149299702	5.56615512246403	30.37408072274598
H	5.05114605867821	5.63342914716831	31.46182733172065
C	8.14057265657534	6.56808754268500	21.30328638695589
H	9.12282852914336	6.28080706249976	20.92339564518143
C	5.44563466797540	11.75983332797894	29.77714196686681
H	5.51480513244075	10.88210209936972	29.12005020867641
H	4.83366188450083	12.51818795516508	29.26670397153446
H	4.90535130390895	11.46216685766984	30.68875891336959
C	3.29488398542191	8.37242205470351	27.48939582917828
H	3.12526718727548	8.69427275584627	28.52803233011637
H	2.55638720503239	8.88309986136633	26.85310497367524
H	4.29858481663437	8.70804180706345	27.18994006030849
C	9.49526898845027	9.37848653473254	31.81753932946239
H	10.15381625159499	8.64167547739911	32.28140474045884
C	10.82913541571979	13.80141695940076	27.12551853171590
C	10.72263985179429	14.04896793408987	28.45837833951209
H	11.09166642714970	15.01322572594295	28.80595306894586
C	1.73604543835990	6.37898748113144	27.69153473225489

H	1.62852385553816	5.29105125086285	27.57182777165266
H	1.00581351603025	6.86977606866229	27.03115336337875
H	1.46507193272365	6.63019020394768	28.72774031736320
C	12.08020577568777	11.58729376464960	25.07217839917595
C	8.19309418725749	9.52167077003963	32.28656540120505
H	7.83331314563806	8.89702386061514	33.10680113826626
C	10.19318952935727	13.19378730800493	29.50226012166081
C	7.45723227782609	2.53609166996639	28.22857889003978
H	7.63030535895950	2.45796862056095	29.31223215080509
H	8.27154849865334	1.99554179434384	27.72363337457938
H	6.51257324409347	2.02018641281702	28.00272350428594
C	3.15289972850787	7.63942828475675	21.72401391916899
H	3.33306494166397	8.27959981995375	20.84763578718469
H	2.17665884256201	7.92280436188335	22.14450441938026
H	3.08451865929907	6.60011268472058	21.37099908713245
C	11.81250202318032	11.60111096322915	22.65232872045299
H	12.18883218929098	11.33871681417808	21.66157527737224
C	10.28069135059773	13.58636392219894	30.80422783542227
H	9.90967794380501	12.98481104066564	31.62967820408744
H	10.74867848466252	14.54075403127510	31.03794040583599
C	4.32544211809824	9.25340462567534	23.29466090966079
H	5.07703579847075	9.35336358859830	24.09159852637888
H	3.35082198909228	9.56523544366330	23.69940143891304
H	4.59346218352376	9.94955001585516	22.48545852209750
C	8.78208933815535	13.40459944627531	24.09170487891562
H	8.51652716516465	13.54725163311247	25.15058189427233
C	6.68527937141103	13.52287673032717	31.08083066858746
H	6.25772360595811	13.18926112333750	32.03948654980739
H	6.00943000160389	14.28145419325505	30.65697040849183
H	7.65508936591891	13.99751383769784	31.27950490227369
C	12.54148126623332	11.26591205416322	23.78954071778429
H	13.49277147673968	10.74189769780036	23.68033330326424
C	8.76136896051179	4.70697499650055	28.05099133136878
H	8.75195309996339	5.73872072125784	27.67008297392830
H	9.58958835260579	4.16819667001430	27.56645857250148
H	8.97045543521860	4.74568263543164	29.13067392399838
C	11.83683691676567	8.54202662884754	30.11653571238368
H	11.81558286050051	7.96161592242921	31.05132301108179
H	12.86309893667626	8.48761148109309	29.72295395132302
H	11.17114665099683	8.05142704953892	29.39271120707231
C	11.42166172728207	14.85782698318099	26.23199554629149
H	12.15825283369421	14.45035309165515	25.52605807001256
H	11.90821823951117	15.62868279687893	26.84114182071805
H	10.64095633901779	15.34489043072409	25.62919488044285
C	7.63039275763056	12.64797559233364	23.40746202133334
H	7.80728100427441	12.55478354257603	22.32495913030391
H	6.68486902884901	13.19366798909799	23.54413851861556
H	7.50312638392482	11.63749861358009	23.81593532598957
C	12.94846729058941	11.23122295148325	26.27498592218447
H	12.32515709516953	11.32566162789137	27.17718431340966
C	12.38523964115773	10.65354860495738	31.38307203845021
H	12.15620892874765	11.71868274655352	31.52025611247923
H	13.43144708257245	10.56406883283751	31.05206057319552
H	12.29679198908787	10.15066022887030	32.35891332980808
C	8.83133073390235	3.72553964540709	22.28365437627571
H	7.92289878395933	3.25165520913920	21.88400372541036
H	9.39322075145881	2.96639473090724	22.84775750316009
H	9.45334744504199	4.03047208632862	21.42893222698349
C	9.76504487951549	5.55413872484442	23.77727307859755
H	10.41244288360918	5.95789046325067	22.98428460885519
H	10.34450959374235	4.80374887734251	24.33587461740527
H	9.51498221139763	6.37680698332211	24.46296987550628
C	8.91768027335686	14.79226816551053	23.43575359058903
H	9.73514994580703	15.38513191289205	23.86614029760136
H	7.98347843792312	15.36142590796928	23.55443662017678
H	9.11395550365062	14.69632028482400	22.35694735754071
C	13.47665343777078	9.78923903275437	26.22505581741856
H	12.66109613503967	9.06343785399141	26.10016555434891
H	14.00167710229958	9.55120011846136	27.16227202648466
H	14.19546420931568	9.64507866793052	25.40441939569680
C	14.12327356349195	12.21565507962175	26.42698869124569
H	14.77287317526423	12.18752403541831	25.53838991983670

H	14.73430942375266	11.94684898422087	27.30180298386289
H	13.77865928454108	13.24891808004947	26.56409384296799

Cartesian coordinates of the optimized gas phase geometry of the complex **3** (PBE/def2-TZVP, S= 0)

Ni	3.46992935601479	8.24848891114341	9.42394021291902
Ni	3.99945139093572	6.50413538060208	7.81811191628061
P	5.43802409058460	8.25154506453334	10.81854611458549
P	4.56181039361306	10.19398197523525	10.12900378103278
P	5.54958207834036	7.89532214133878	8.52478539023505
P	3.33021560240204	7.25291596799215	11.61208141382603
P	1.95928025350554	8.86440610564872	11.03495165267339
P	1.98769244389277	7.42772188551576	7.94189049390136
Si	6.19775518786027	10.08590306182417	8.59125307813643
P	3.03811412892156	5.85559703933306	9.76398130776037
P	0.92025785582594	5.92504414723546	9.19025352326131
Si	0.17882377280012	7.45958588247207	10.74315362369082
N	7.91835691136872	10.25101080937710	8.92771041929245
N	5.94524775562550	11.25223961616107	7.29714716796257
N	4.66270746557256	3.82708029602057	6.80730040053223
N	4.07596441236421	5.11155268750884	5.17535444381488
N	-0.35251256947311	6.66204958938008	12.23807110575826
N	-1.29048766039089	8.27048312199405	10.19762943542857
C	8.31791876215020	11.58999752164214	6.90637987306788
H	9.07811065361695	11.99787788315683	6.24062275214401
C	8.46995513236494	9.54734096977946	10.06072947224468
C	8.41850732214850	10.14485981765447	11.33799795865046
C	7.02052353217213	11.76020526796878	6.54140873502059
C	8.83136311988285	10.97134402647939	8.11676136638077
C	9.09648379431490	8.29609648385081	9.86572197145038
C	0.59330717355261	6.24718152304036	13.24823486824612
C	4.24541542037167	5.11406528264357	6.53988442820260
C	9.23017649433681	7.69380439232699	8.49454867978549
C	8.95374378505459	9.44243518335806	12.42662673714601
H	8.91282618198720	9.89631145122093	13.41935567285490
C	6.23209553027205	3.45777588130764	8.65390979784171
C	7.82446842625212	11.51180187477121	11.54056434766739
C	4.75190712244003	3.06648520350602	5.64842953918348
H	5.07137626116299	2.03136095612851	5.66637540030904
C	4.95153557134074	3.27184783908229	8.10583029077409
C	4.67381425801164	11.93522382423819	7.20672519774513
C	3.79740810554365	10.09089671976678	5.70179203765313
C	3.62862511544296	11.38745500039146	6.43741015413357
C	4.51808828244569	13.16731328547652	7.88106781833575
C	3.95368536175127	2.51328847600257	8.74443684317723
C	10.15018805741364	11.09117702214225	8.43348286001411
H	10.58200493106136	10.66035181404718	9.33369022313237
H	10.80527804408264	11.65039034260954	7.76844484192579
C	5.62995568083753	13.75078999678194	8.71054878756912
C	9.61742947626346	7.63063666538721	10.98178195452914
H	10.09746987434477	6.65928147867487	10.84070639227881
C	7.29262794536191	4.23569304484085	7.92611455156622
C	4.38250295988599	3.87313081377325	4.62163354441219
H	4.31235356914549	3.69032967516730	3.55604010975853
C	9.54093092563170	8.19154042396075	12.25590838523667
H	9.95148870577263	7.65753030730043	13.11489551556647
C	6.07969841438344	6.89122444809674	4.12343559984853
C	4.62413512064707	7.03901158143874	3.77238671840387
C	6.67478491544051	12.52114129048097	5.29008933549736
H	6.03559606193510	11.92592305600115	4.61970485788666
H	7.59072527664939	12.79422201731720	4.75266357292929
H	6.11826788859180	13.44391998797047	5.51510292173181
C	3.64511908779630	6.20750560649312	4.34459931835980
C	1.15935235455759	4.95560535240541	13.22238696962057
C	2.39458607186821	5.49241429409397	15.25072136878633
H	3.10374913623561	5.20005762632715	16.02727208478739
C	-1.21612280510547	9.26236963658676	9.14958375256752
C	3.29582837186696	13.84095649922917	7.76737146036496
H	3.16711592908399	14.79396409043817	8.28581294765775
C	2.59311045753372	2.32254487166951	8.13159780676526
C	6.48994547192097	2.88761348009227	9.90736192896030
H	7.47377242313162	3.02935069673223	10.35915813251260
C	4.26319594510977	1.95477300325269	9.99084843530459

H	3.50238357319896	1.36781719083663	10.50967556851989
C	-1.03179468548414	10.61634839596460	9.50637024378026
C	5.51551335074401	2.14617496275781	10.57243229047188
H	5.73544953256485	1.70965844509765	11.54825649134192
C	2.41922431262970	12.09011272293929	6.36026656945946
H	1.59983868982583	11.66461285029849	5.77786349200931
C	0.89631454803634	7.15149012284907	14.29440353330113
C	2.06516285027838	4.60255385424746	14.23433185020166
H	2.51037228716587	3.60473931955749	14.21768348938735
C	4.19520542240781	8.01481158277493	2.86403736927009
H	4.93676923932244	8.67088541225609	2.40350684306077
C	2.27583026016973	6.32767560265333	4.04812682956313
C	1.25466761212881	5.41410808978077	4.66784854790697
C	2.84464004111743	8.15781525009766	2.54991897634044
H	2.52945865068256	8.92444367679069	1.83982122321137
C	1.89527713093682	7.32761398590185	3.14354248102227
H	0.83721158213261	7.44407557938107	2.90019761689878
C	0.82178510769384	3.93851590248659	12.16398542738922
C	2.25091620106568	13.30729027860133	7.01549041450496
H	1.30151845586896	13.84116781025367	6.94271298256785
C	-1.72042470434779	6.44993458202417	12.49964356624129
C	1.80507814327490	6.75611462177416	15.28132143365424
H	2.04786869126308	7.45314343971763	16.08652737360059
C	-0.93985225427282	11.04451266990933	10.94605473939897
C	0.25969690744747	8.51315515010991	14.35534313277780
C	-2.59081454318014	7.97805547463608	10.68160412866780
C	-1.38911377740464	9.88185067102083	6.82008083132104
H	-1.55997330463528	9.59947014010445	5.77841780869356
C	-1.43515128790326	8.88649103549922	7.80590651907534
C	-2.71115957882509	7.02078273725284	11.76450247425228
H	-3.73453055014770	6.77017460781433	12.04101618740744
C	-0.99087367204020	11.57573775780120	8.48700498031152
H	-0.84273121591943	12.62392711324315	8.75601296938574
C	-2.07170841448027	5.54610134518581	13.65108738112157
H	-1.64435790915826	4.53931644101767	13.52781771919434
H	-3.16139721163083	5.45496691124431	13.72855733393954
H	-1.68749932922261	5.93449241835319	14.60675035804782
C	-3.70910825104113	8.57583043642078	10.18340425816843
H	-3.68220856058039	9.31321641000346	9.38529691728951
H	-4.67659520159823	8.32161813766952	10.61180758215770
C	-1.15889781328493	11.21451815060678	7.15215154745067
H	-1.13514720923045	11.97729647095877	6.37110058298687
C	-1.77466307405937	7.47151145707219	7.42023655320214
H	0.62173628417346	9.15711206884774	13.53714131902252
H	-0.83471707132173	8.46271643196355	14.25623957787775
H	0.50142095432538	9.00934873518965	15.30439710877910
H	0.63253564178636	2.95624010848339	12.62263759965502
H	-0.05763890736069	4.22228080401074	11.57422343357774
H	1.66186545903586	3.80981327140906	11.46170250884641
H	-0.89031368637709	6.81483483441701	7.43749601707643
H	-2.51776761927018	7.03949533388831	8.10497005964896
H	-2.18501466243520	7.44433917636976	6.40146435960109
H	0.01683901703649	10.74382437024811	11.40165630010324
H	-1.01635205326333	12.13713665045987	11.02465534283358
H	-1.74519643547853	10.59397118406766	11.54402352927781
H	7.47879952172722	3.82745625602253	6.92084682239098
H	6.99143417092665	5.28678966120053	7.79868304024160
H	8.23718560525024	4.21543395685742	8.48402289617946
H	2.64922138466736	1.85941231339860	7.13491167666725
H	1.97074965363167	1.68168716698461	8.76887473843228
H	2.07338769990181	3.28640933030244	8.01206989547824
H	1.44422903935501	4.35927093474100	4.41557887291643
H	1.27057107778604	5.49123891338691	5.76584661567284
H	0.24582942331580	5.67065562311349	4.32096648911068
H	6.68587038447577	7.62613354203288	3.57906392766407
H	6.24172952309925	7.04084869010975	5.20215204641253
H	6.46063455790751	5.88755080289535	3.87964476819556
H	8.18020213759558	12.21903198872817	10.77789660253789
H	6.72360278643056	11.48639542475399	11.47640558123149
H	8.08913385273479	11.90330131241577	12.53179051235173
H	9.78295599231105	6.74611235222298	8.54107384876029
H	8.24504339294198	7.49215333194355	8.04465042577434

H	9.76160535229059	8.37690451841043	7.81491001202126
H	6.54618298432566	13.91542056621985	8.12295081211379
H	5.32289191242751	14.71045972550698	9.14625665362460
H	5.90838238567164	13.07780603005748	9.53672435315346
H	4.69595423186427	10.09605714597483	5.06768118333333
H	3.91037642877044	9.24432623798799	6.39767471911179
H	2.92751097040386	9.88572031999116	5.06597393068944

5 References

1 M. R. Elsby and S. A. Johnson, *J. Am. Chem. Soc.*, 2017, **139**, 9401.
2 a) M. R. Elsby, J. Liu, S. Zhu, L. Hu, G. Huang and S. A. Johnson, *Organometallics*, 2019, **38**, 436; b) D. Wang, X. Leng, S. Ye and L. Deng, *J. Am. Chem. Soc.*, 2019, **141**, 7731.
3 M. Driess, S. Yao, M. Brym, C. van Wüllen and D. Lentz, *J. Am. Chem. Soc.*, 2006, **128**, 9628.
4 Y. Xiong, S. Yao, M. Brym and M. Driess, *Angew. Chem. Int. Ed.*, 2007, **46**, 4511.
5 P. H. M. Budzelaar, *gNMR for Windows (5.0.6.0), NMR Simulation Programm*, *2006*.
6 a) SCALE3ABS, CrysAlisPro, Aglient Technologies Inc. Oxford, GB, 2015; b) G. M. Sheldrick, SADABS, Bruker AXS, Madison, USA, 2007.
7 R. C. Clark, J. S. Reid, *Acta Crystallogr. A*, 1995, **51**, 887.
8 O. V. Dolomanov, L. J. Bourhis, R. J. Gildea, J. A. K. Howard, H. Puschmann, *J. Appl. Cryst.* 2009, **42**, 339.
9 G. M. Sheldrick, *Acta Cryst.*, 2015, **A17**, 3.
10 G. M. Sheldrick, *Acta Cryst.*, 2015, **C71**, 3.
11 Y. Xiong, S. Yao, E. Bill and M. Driess, *Inorg. Chem.*, 2009, **48**, 7522.
12 G. Prabusankar, A. Doddi, C. Gemel, M. Winter and R. A. Fischer, *Inorg. Chem.*, 2010, **49**, 7976.
13 J. W. Dube, C. M. E. Graham, C. L. B. Macdonald, Z. D. Brown, P. P. Power and P. J. Ragogna, *Chem. Eur. J.*, 2014, **20**, 6739.
14 O. J. Scherer, M. Swarowsky, H. Swarowsky and G. Wolmershäuser, *Angew. Chem. Int. Ed. Engl.*, 1988, **27**, 694.
15 F. Neese, *Wiley Interdiscip. Rev. Comput. Mol. Sci.*, 2012, **2**, 73.
16 F. Weigend, *Phys. Chem. Chem. Phys. 2002*, **4**, 4285
17 F. Neese, F. Wennmohs, A. Hansen, U. Becker, *Chem. Phys.*, 2009, **356**, 98.
18 Perdew, Burke and Ernzerhof, *Phys. Rev. Lett.*, 1996, **77**, 3865.
19 F. Weigend, R. Ahlrichs, *Phys. Chem. Chem. Phys.*, 2005, **7**, 3297.
20 F. Weigend, *Phys. Chem. Chem. Phys.*, 2006, **8**, 1057.
21 E. D. Glendening, C. R. Landis, F. Weinhold, *J. Comput. Chem.*, 2013, **34**, 1429.
22 Gaussian 09, Revision E.01, M. J. Frisch, G. W. Trucks, H. B. Schlegel, G. E. Scuseria, M. A. Robb, J. R. Cheeseman, G. Scalmani, V. Barone, G. A. Petersson, H. Nakatsuji, X. Li, M. Caricato, A. Marenich, J. Bloino, B. G. Janesko, R. Gomperts, B. Mennucci, H. P. Hratchian, J. V. Ortiz, A. F. Izmaylov, J. L. Sonnenberg, D. Williams-Young, F. Ding, F. Lipparini, F. Egidi, J. Goings, B. Peng, A. Petrone, T. Henderson, D. Ranasinghe, V. G. Zakrzewski, J. Gao, N. Rega, G. Zheng, W. Liang, M. Hada, M. Ehara, K. Toyota, R. Fukuda, J. Hasegawa, M. Ishida, T. Nakajima, Y. Honda, O. Kitao, H. Nakai, T. Vreven, K. Throssell, J. A. Montgomery, Jr., J. E. Peralta, F. Ogliaro, M. Bearpark, J. J. Heyd, E. Brothers, K. N. Kudin, V. N. Staroverov, T. Keith, R. Kobayashi, J. Normand, K. Raghavachari, A. Rendell, J. C. Burant, S. S. Iyengar, J. Tomasi, M. Cossi, J. M. Millam, M. Klene, C. Adamo, R. Cammi, J. W. Ochterski, R. L. Martin, K. Morokuma, O. Farkas, J. B. Foresman, and D. J. Fox, *Gaussian, Inc., Wallingford CT*, 2009.
23 G. Knizia, *J. Chem. Theory Comput.*, 2013, **9**, 4834.
24 J. Tao, J. P. Perdew, V. N. Staroverov and G. E. Scuseria, *Phys. Rev. Lett.*, 2003, 91, 146401.
25 F. Jensen, *J. Chem. Theory Comput.*, 2015, **11**, 132.